Pharmacology and Therapeutic Potential of Benzothiazole Analogues for Cocaine Use Disorder

Comfort A. Boateng,[†,#,] Ashley N. Nilson,[≠#] Rebekah Placide,[†] Mimi L. Pham,[†] Franziska M. Jakobs,[†] Noelia Boldizsar,[≠] Scot McIntosh,[†] Leia S. Stallings,[†] Ivana V. Korankyi,[†] Shreya Kelshikar,[+] Nisha Shah,[+] Diandra Panasis,[+] Abigail Muccilli,[+] Maria Ladik,[+] Brianna Maslonka,[+] Connor McBride,[+] Moises Ximello Sanchez,[+] Ebrar Akca,[+] Mohammad Alkhatib,[+] Julianna Saez,[+] Catherine Nguyen,[+] Emily Kurtyan,[+] Jacquelyn DePierro,[+] Raymond Crowthers,[+] Dylan Brunt,[+] Alessandro Bonifazi,[^] Amy Hauck Newman,[^] Rana Rais,[‡] Barbara S. Slusher,[‡] R. Benjamin Free,[≠] David R. Sibley,[≠] Kent D. Stewart,[†] Chun Wu,[+] Scott E. Hemby,[†] Thomas M. Keck[+,*]*

[†]Department of Basic Pharmaceutical Sciences, Fred Wilson School of Pharmacy, High Point University, One University Parkway, High Point, North Carolina, 27268, United States

[+]Department of Chemistry & Biochemistry, Department of Biological & Biomedical Sciences, College of Science and Mathematics, Rowan University, 201 Mullica Hill Road, Glassboro, New Jersey, 08028, United States

[^]Medicinal Chemistry Section, Molecular Targets and Medications Discovery Branch, National Institute on Drug Abuse-Intramural Research Program, National Institutes of Health, 333 Cassell Drive, Baltimore, Maryland, 21224, United States

[‡]Department of Neurology, Johns Hopkins Drug Discovery, The Johns Hopkins University School of Medicine, 855 N. Wolfe Street, Baltimore, MD 21205, United States

[≠]Molecular Neuropharmacology Section, National Institute of Neurological Disorders and Stroke-Intramural Research Program, National Institutes of Health, Bethesda, Maryland, 20892, United States

[#] Equally Contributing Authors, * Corresponding Authors

KEYWORDS. Dopamine D_4 receptor, antagonist, phenylpiperazine, benzo[*d*]thiazole, cocaine abuse disorder

ABSTRACT

The dopamine D_4 receptor (D_4R), a G protein-coupled receptor, is predominantly expressed in brain regions that control cognition, attention, and decision making. Previous studies have indicated that D_4R-targeted ligands could be promising therapeutic targets for the treatment of several neuropsychiatric conditions, including substance use disorders (SUDs). There are currently no FDA-approved medications that selectively target D_4Rs. New ligands may facilitate better understanding of the role of D_4R-mediated signaling in drug-taking and drug-seeking behaviors. The present study focuses on the synthesis and evaluation of a novel series of benzothiazole analogues designed to target D_4R. We identified several compounds with high D_4R binding affinity ($K_i \leq 6.87$ nM) and >91-fold selectivity over other D_2-like receptors (D_2R, D_3R) with diverse partial agonist and antagonist profiles. Based on receptor affinity and functional analyses, **5f** was identified as a potent low-efficacy partial agonist of the D_4R and selected for further investigation. **5f** was metabolically stable in rat and human liver microsome assays and displayed excellent brain penetration in rats. Using a within-session multidosing procedure, **5f** (5, 15 and 30 mg/kg, i.p.) dose-dependently decreased i.v. infusions of three-unit doses of cocaine under a fixed-ratio (FR) FR3 schedule of reinforcement. These results are consistent with previous results produced by D_4R-selective antagonists in SUD models, however off-target antagonism of 5-HT_{2A} or 5-HT_{2B} receptors may also contribute to these effects. Results with compound **5f** support further efforts to target D_4R in the treatment of SUDs. Further development of the benzothiazole scaffold may engineer out any serotonergic activity.

INTRODUCTION

D_1-like (D_1R, D_5R) and D_2-like (D_2R, D_3R, D_4R) dopamine receptors are G protein-coupled receptors that regulate physiological functions such as movement, emotion, and cognition.[1, 2] Compared to D_2R and D_3R, D_4Rs have the lowest level of expression in the brain, and are uniquely distributed primarily in the prefrontal cortex and hippocampus. In the prefrontal cortex, D_4R plays important roles in cognition, attention, decision making, and executive function. Studies with D_4R-selective ligands demonstrate that the D_4R is a promising therapeutic target for the treatment of several neuropsychiatric conditions, including attention deficit-hyperactivity disorder (ADHD) and substance use disorders (SUDs).[3, 4] D_4R ligands alter cognition and behavior in animal models of drug addiction and common variations in the *DRD4* gene are associated with novelty-seeking, risky behavior, ADHD, and SUDs.[5] A better understanding of D_4R-mediated signaling is essential to developing new pharmacotherapeutic treatments.

D_4R antagonism may be useful to treat both L-DOPA-induced dyskinesias and SUDs (particularly for psychostimulants like cocaine;[4, 6-8]). Despite the clinical implications of cocaine use disorder (CUD), there are no FDA-approved medications for CUD treatment or approved drugs that selectively target D_4R. One of the most well-studied D_4R-selective compounds, L-745,870 (**1**; 3-(4-[4-chlorophenyl]piperazin-1-yl)-methyl-1*H*-pyrrolo[2,3-*b*]pyridine; **Figure 1**) is >100-fold selective for D_4R over other dopamine receptors (D_1R, D_2R, D_3R, and D_5R) with sub-nanomolar affinity.[9, 10] However, the compound acts as a partial agonist, binds to several non-dopaminergic receptors, and failed to reduce psychotic symptoms in a Phase IIa clinical study evaluating its utility as an antipsychotic.[11, 12]

The goal of this study was the development and characterization of novel ligands with high D_4R affinity and selectivity for investigation in rodent models of CUD. Compound **5a** (2-(4-(4-(pyrimidin-2-yl)piperazin-1-yl)butyl)benzo[*d*]thiazole; **Figure 1**) was identified in a prior drug development study as a compound with high D_4R affinity and selectivity over D_2R and D_3R, with close analogues having useful effects in treating sexual dysfunction.[13, 14] We used **5a**[13] as the chemical template for two rounds of structure-activity relationship (SAR) guided synthesis, with the goal of identifying novel druggable D_4R-selective lead compounds.

We synthesized an initial library of analogues (**5b**-**5f**) featuring modifications to the pyrimidinylpiperazine region of **5a** and variations in the linker chain length. Following extensive *in vitro* analyses, including binding and functional studies, we determined that these modifications resulted in several novel analogues that retained high D_4R binding affinity, improved D_2-like subtype selectivity, and low-efficacy partial agonist or antagonist profiles at D_4R. Based on its initial profile, we expanded the characterization of **5f** to include diverse receptor screening, pharmacokinetic and metabolic stability studies, including rat and human liver microsomes, and *in vivo* behavioral analysis in rats trained to self-administer cocaine. In parallel with the *in vivo* characterizations of **5f**, we pursued a second round of SAR studies exploring substitutions on both the terminal benzo[*d*]thiazole and the pyrimidine/pyridine scaffolds as well as piperazine versus piperidine moieties, as identified in an *in silico* screen using a the D_4R crystal structure (crystalized with the antipsychotic nemonapride **2** (**Figure 1**) modified via molecular docking.[15] These diverse libraries provide valuable insight into the structure activity relationship driving D_4R ligand affinity, efficacy, and target selectivity.

CHEMISTRY

Ligands were synthesized as outlined in **Scheme 1** using routine N-alkylation reactions previously reported.[2] In **Scheme 1**, substituted or unsubstituted 2-aminobenzenethiol compound **3** or **7** was reacted with 4-chlorobutanoyl chloride or 5-chloropentanoyl chloride to give the cyclized intermediates **4** or **8**. Alkylation of the substituted or unsubstituted arylpiperazine or arylpiperidine moiety with intermediate compound **4**, delivered target compounds **5** and **6**. The same procedure was employed to make target compounds **9** and **10** starting from **8**. The requisite substituted or unsubstituted aminothiophenols and substituted or unsubstituted arylpiperazines or arylpiperidines are commercially available.

PHARMACOLOGICAL RESULTS AND DISCUSSION

Structure-Activity Relationships at Dopamine D_2-Like Receptors: Initial Library.

A primary objective of this study was to design ligands with high D_4R binding affinity and D_2-like subtype selectivity for the treatment of CUD. Compound **5a** and the structures of all synthesized analogues are shown in **Table 1**. In an initial small SAR study, we employed two classes of modifications to parent compound **5a**, varying alkyl linker chain length and substitutions on the arylpiperazine. A small initial analogue library was synthesized (**5b-5f**) with one compound (**5f**) chosen for further investigation. This library was later extended (**5g-h**, **6a-b**, **9a-d**, **10a-c**) on the basis of *in silico* docking studies, described below. This extended library featured additional arylpiperazine/arylpiperidine substitutions as well as modifications to the benzo[*d*]thiazole. Overall, all compounds exhibited cLogP values of less than 5 and each member of the extended library demonstrated higher binding affinity for D_4R than D_2R and D_3R.

The 2-pyrimidine moiety of **5a** was replaced with a 2-pyridine in **5b**, 5-methylpyridin-2-yl in **5c** and 5-chloropyridin-2-yl in **5d**. To evaluate the contribution of the alkyl chain to binding affinity

and subtype selectivity, we synthesized alkyl chain length analogues of compounds **5a** and **5b**, removing one methylene from the linker chain in compounds **5e** and **5f**, respectively. The pyridine of compound **5f** was substituted with a 4-methylpyridin-2-yl to form **5g**. The piperazine attached to the three-C-linker chain on compound **5h** with 3-methoxy-2-pyridinyl moiety was replaced with a piperidine to form **6a** with 3-methyl-2-pyridinyl moiety. The 3-methyl-2-pyridine of **6a** was substituted with a 5-methoxy-2-pyridine to form **6b**. Finally, we probed the contribution of the benzo[*d*]thiazole moiety via substitution on the phenyl ring with electron donating (methyl) and withdrawing (chloro) groups (compound **9a** compared to compound **9b**, respectively) with a propyl linker attached to pyridin-2-yl-piperazin-1-yl moiety. Additional substitutions on the benzo[*d*]thiazole moiety produced compounds **9c-9d**. We also probed combinations of benzo[*d*]thiazole moiety substitutions with pyridin-2-ylpiperidin-1-yl moieties attached to the propyl linker to obtain compounds **10a-10c**. Synthetic procedures for all compounds are shown in **Scheme 1** and final structures for each compound are shown in **Table 1**.

The binding affinities of all compounds were evaluated via radioligand competition binding studies using [^{3}H]*N*-methylspiperone and membranes prepared from HEK293 cells stably expressing human dopamine D_2-like receptors (D_2R, D_3R, or D_4R). Binding data for all ligands are shown in **Table 1**. In addition, cLogP and polar surface area (PSA) values were calculated to provide measures of lipophilicity (**Table 1**). Functional analyses of each compound were completed using the LANCE assay for cAMP (**Table 2**) and the DiscoverX β-arrestin recruitment assay (**Table 3**), both in agonist and antagonist modes, using Chinese hamster ovary (CHO) cells stably expressing D_2R, D_3R, or D_4R. In agonist mode, E_{max} values for each compound are in comparison to dopamine and EC_{50} values represent agonist potency. In antagonist mode, I_{max}

values for each compound represent inhibition of dopamine-induced signaling and IC_{50} values represent antagonist potency.

Modification of the pyrimidine ring of **5a** to a pyridine or substituted pyridine (**5b**-**5d**) modestly decreased D_4R binding affinity in competition binding assays and decreased fold selectivity over the structurally related D_3R. Compounds **5b** and **5c** had decreased but still highly potent D_4R binding affinity at 9.85 ± 2.01 nM and 21.2 nM ± 1.37, respectively. The D_2R/D_4R fold selectivity was similar to compound **5a** at ~40-fold but the D_3R/D_4R fold selectivity decreased to 6-fold (**5b**) and 10-fold (**5c**). In cAMP antagonism assays, **5b** and **5c** were full antagonists (~100% inhibition) at D_4R but lost potency to (IC_{50} = 123 nM [95.9 – 157] and 600 nM [467 – 771], respectively) compared to **5a** (IC_{50} = 31.8 nM [24.7 – 40.9]). Further, **5b** inhibited cAMP production via activation of the D_2R (E_{max} = 59.4 ± 3.0%, EC_{50} = 124 nM [68.9 – 222]) while the methyl substitution in **5c** remained inactive in agonist mode but was a full D_2R antagonist with low potency (I_{max} = 107 ± 5, IC_{50} = 2010 [1390 – 2910]). Similar results for the D_4R and D_2R were seen in the β-arrestin assay. **5b** was a full antagonist at the D_4R (I_{max} = 97.8 ± 3.6%, IC_{50} = 104 nM [71.7 – 153]) but was a partial agonist at the D_2R (E_{max} = 32.0 ± 0.9%, EC_{50} = 29.8 nM [18.6 – 47.6]). Additionally, **5b** was a potent agonist at the D_3R for β-arrestin recruitment (E_{max} = 82.6 ± 5.3, EC_{50} = 17.8 nM [7.34 – 43.1]. As with the cAMP assay, addition of the methyl substituent in **5c** removed any agonist activity in the β-arrestin recruitment assay. **5c** was a full antagonist at the D_2R (I_{max} = 104 ± 4%, IC_{50} = 1560 nM [1120 – 2170]), D_3R (I_{max} = 101 ± 8%, IC_{50} = 937 nM [541 – 1630]), and D_4R (I_{max} = 108 ± 4%, IC_{50} = 275 nM [185 – 408]) but did not show high selectivity amongst the receptors (< 6-fold). Replacing the pyrimidine ring with a pyridine ring introduced D_2R and D_3R partial agonist activity while adding a methyl substituent to the pyridine ring restored full antagonism at all receptors.

The chloro-substituted pyridine **5d** maintained high D_4R binding affinity (K_i = 4.85 ± 0.57 nM) with decreased D_2R affinity (K_i = 830 ± 160 nM) compared to **5a** (K_i = 127 ± 10 nM), which improved D_4R selectivity over D_2R to 171-fold. **5d** maintained similar D_3R binding affinity as **5a** and thus had no improvement in D_4R selectivity over D_3R. However, cAMP and β-arrestin recruitment were greatly diminished across all receptors. Starting with the D_4R, **5d** lost potency in cAMP assays with the estimated IC_{50} = 10,800 nM [7520 – 15,500]. In the β-arrestin assay, **5d** was a full antagonist (I_{max} = 103 ± 4%, IC_{50} = 414 nM [274 – 621]). At the D_2R, **5d** had greatly reduced potency at both cAMP (I_{max} and IC_{50} = Not determined) and β-arrestin recruitment (I_{max} = 108 ± 19%, IC_{50} = 23,000 nM [8960 – 67,700]). **5d** did not recruit β-arrestin to the D_3R indicating no detectable agonist activity and very low potency antagonism was suggested but accurate potency was not determined due to incomplete (unsaturated) curves. Although D_4R binding affinity was not affected by the chloro substituent, functional activity was greatly diminished for all D_2-like receptors.

Removing one methylene unit from the linker chain—decreasing the alkyl linker from four carbons to three—markedly improved selectivity for D_4R by reducing D_2R and D_3R binding affinities. Compared to similar butyl linker compounds **5a**-**5c**, the propyl linker chain in **5e**-**5g** maintained D_4R binding affinity and greatly reduced D_2R and D_3R binding affinity. For example, **5e** had a D_4R binding affinity (K_i = 6.52 ± 0.61 nM) similar to that of **5a** (K_i = 3.05 ± 0.16 nM) but dramatically decreased affinity for D_2R (**5e**: K_i = 6370 ± 1020 nM; **5a**: K_i = 127 ± 10 nM) and D_3R (**5e**: K_i = 1650 ± 120 nM; **5a**: K_i = 93.2 ± 8.3 nM). Exchanging the pyrimidine in **5e** for a pyridine in **5f** improved D_4R binding affinity (K_i = 2.21 ± 0.01 nM) and further increased D_4R selectivity over both D_2R (1326-fold) and D_3R (520-fold). In cAMP functional assays, **5e** (E_{max} = 14.0 ± 0.8%, EC_{50} = 4.34 nM [1.1 – 17.1]) and **5f** (E_{max} = 14.2 ± 1.2%, EC_{50} = 10.6 nM [1.6 –

64.8]) exhibited low partial agonism at the D_4R, corresponding antagonist mode assays in which **5e** (I_{max} = 82.2 ± 2.0%, IC_{50} = 32.3 nM [24.7 – 42.2]) and **5f** (I_{max} = 78.8 ± 2.3%, IC_{50} = 69.3 nM [50.9 – 94.5]) were partial antagonists. Higher efficacy but much lower potency for **5e** and **5f** were observed at the D_2R in both agonist and antagonist modes. The potency of **5e** at the D_2R was >100,000 nM in antagonist mode. In agonist mode at the D_2R, **5e** was a high efficacy partial agonist (E_{max} = 80.9 ± 6.9%, EC_{50} = 1180 nM [577 – 2390]) with significant D_4R selectivity (272-fold). The D_4R selectivity of **5f** was 97-fold over the D_2R in antagonist mode due to decreased D_2R potency (I_{max} = 81.3 ± 4.5%, IC_{50} = 6690 nM [4120 – 11,000]).

In silico screening to guide SAR library expansion

*Combinatorial library of compound **5f**.* Structural variations of initial lead compound **5f** template were generated, producing a permutational library of 4400 D_4R ligands in total, as shown in **Figure S1**. Individual libraries were built for each core variance shown with simple substitutions using the Combinatorial Library Enumeration tool in Maestro software (Schrödinger): scaffold 1: 6x6x6x6 (1296); scaffold 2: 4x4x4x4x2(512); scaffold 3: 6x6x6x6x2 (2592).

Preparation of Protein and Ligand Library. The crystal structure (5WIU) of the D4R in complex with nemonapride **2** (chemical structure shown in **Figure 1**)[15] was prepared and preprocessed using Maestro's Protein Preparation Wizard.[16] The preprocessed protein's charge state was optimized at pH 7.4. Then a restrained minimization was performed to relax the protein structure using OPLS3 force field.[17] Using Maestro Elements allowed the preparation of the 3D structures of nemonapride **2** and the 4400 **5f** analogues. The 3D structure of nemonapride was extracted from the crystal structure (PDB ID: 5WIU) and the initial structure of the **5f** analogues was from the Combinatorial Library Enumeration tool. In order to generate each ligand's ionization/tautomeric states at pH 7.4, Maestro's Epik tool was used based on the more accurate Hammett and Taft

methodologies.[16] During this step, the lowest ionization/tautomeric state was chosen. Afterwards, the geometry was minimized to the most energetically favorable structure to relax the ligand's structure.

Glide XP Docking and Compound Selection. The receptor grid files were generated from the prepared receptor complex, in which the centroid of the crystal ligand, nemonapride, was used to specify the active site. The prepared ligands were docked into their corresponding generated grids using Glide XP scoring with default procedures and parameters.[17] In detail, the receptor grid required for the docking process was generated using van der Waals scaling factor of 1 and a partial charge cutoff of 0.25. Docking was performed using a ligand-centered grid and OPLS3 force field. Glide XP Dock performed a comprehensive systematic search for the best receptor conformations and orientations to fit the ligand. The docked pose of the crystal ligand was confirmed with its crystal pose, thus validating the docking protocol. Following Glide XP docking, we selected several compounds per library, focusing on compounds with the simplest substitutions while still maintaining improved docking scores relative to the lead scaffold. **Table S2** represents the ten identified ligands with desirable docking scores and with the greatest synthetic feasibility. Both interaction diagrams (left) and 3D representations with interacting residues (right) are provided for the best selected candidate in each of our list.

Structure-Activity Relationships at Dopamine D_2-Like Receptors: Expanded Library.

Adding a 4-methyl substituent onto the pyridine ring (**5g**) maintained high D_4R affinity (K_i = 2.89 ± 0.95 nM) and subtype selectivity of >450-fold over both D_2R and D_3R, with no agonist activity detected for any receptor in either cAMP or β-arrestin recruitment assays. At the D_4R, **5g** was potently antagonized cAMP inhibition (I_{max} = 88.0 ± 4.4%, IC_{50} = 27.8 nM [15.3 – 49.2]) and β-arrestin recruitment (I_{max} = 88.6 ± 4.6%, IC_{50} = 6.18 nM [2.59 – 17.6]). **5g** antagonized D_2R-

mediated cAMP inhibiting (I_{max} = 92.8 ± 4.9%, IC_{50} = 628 nM [375 – 1040]) but was less potent at inhibiting β-arrestin recruitment to the D_2R (I_{max} = 102 ± 6%, IC_{50} = 6430 nM [4010 – 10,300]) and D_3R (I_{max} = 101 ± 10%, IC_{50} = 12900 nM [7490 – 22,400]) compared to its potency at the D_4R.

The 3-methoxy substitution on the pyridine ring (**5h**) improved D_4R-subtype selectivity in binding affinity and β-arrestin recruitment antagonism but not for cAMP inhibition antagonism. **5h** maintained D_4R binding affinity (K_i = 1.74 ± 0.58 nM) but had decreased D_2R (K_i = 519 ± 211 nM) and D_3R (K_i = 288 ± 194 nM) binding affinity. Further, **5h** had >190-fold selectivity for the D_4R in β-arrestin recruitment antagonism. **5h** was inactive for all receptors tested in agonist mode but was highly potent for D_4R-mediated β-arrestin recruitment inhibition (I_{max} = 91.7 ± 3.6%, IC_{50} = 2.17 nM [1.41 – 3.40]). **5h** was much less potent for β-arrestin recruitment inhibition at the D_2R (I_{max} = 94.0 ± 3.6%, IC_{50} = 414 nM [268 – 633]) and D_3R (I_{max} = 81.5 ± 3.4%, IC_{50} = 474 nM [298 – 747]). Interestingly, D_4R-subtype selectivity was lost in cAMP functional assays. **5h** was inactive as an agonist at both the D_2R and D_4R but had similar potency D_4R-mediated cAMP inhibition antagonism (I_{max} = 90.4 ± 2.6%, IC_{50} = 30.6 nM [23.1 – 40.6]) when compared to **5a**. The potency of **5h** for D_2R-mediated cAMP inhibition antagonism was 185 nM [105 – 327] (I_{max} = 86.4 ± 4.4). Together, these results indicate the importance of the propyl linker length on D_4R affinity and subtype selectivity. Further, substitutions on the pyridin-2-yl-piperazin-1-yl moieties can dramatically alter the intrinsic efficacy of each compound.

We probed the importance of the piperazine ring by replacing it with a piperidine in compounds **6a** and **6b**. While we lack matching piperazine analogues, comparing **6a** and **6b** to the **5a-h** series shows a loss of D_4R binding affinity (K_i = 24-26 nM) but excellent selectivity over D_2R (>500-fold) due to a marked reduction in D_2R binding affinity. In functional assays, **6a** was a full

antagonist at the D_4R (cAMP: I_{max} = 97.6 ± 4.5%, IC_{50} = 67.2 [41.2 – 109]; β-arrestin: I_{max} = 100 ± 2%, IC_{50} = 52.4 nM [40.3 – 68.3]) and had lower potency at the D_2R (cAMP: I_{max} = 104 ± 6%, IC_{50} = 4530 nM [2740 – 7500]; β-arrestin: I_{max} = 100 ± 2%, IC_{50} = 9920 nM [7660 – 12,900]) and D_3R (β-arrestin: I_{max} = 101 ± 2%, IC_{50} = 13,300 nM [9450 – 18,700]). **6b** was an antagonist in cAMP and β-arrestin recruitment assays for all receptors tested but did not maintain selectivity for D_4R over D_2R compared to **6a** (cAMP: 14-fold; β-arrestin: 43-fold) or D_3R (β-arrestin: 25-fold selective).

The benzo[*d*]thiazole moiety represents a new secondary pharmacophore for the arylpiperazine/ arylpiperidine class of D_2-like ligands. We evaluated the suitability of modifying this region of the molecule by adding electron donating and withdrawing groups onto the phenyl ring, producing mixed effects on binding affinity. 6-Methylbenzo[*d*]thiazole (**9a**) and 6-chlorobenzo[*d*]thiazole (**9b**) both reduced D_4R binding affinity (K_i = 59.0 ± 45.4 nM and K_i = 27.2 ± 10.0 nM, respectively) compared to the unsubstituted analogue **5f** (K_i = 2.21 ± 0.01 nM). While the electron-donating methyl group on **9a** produced excellent selectivity over D_2R (844-fold) and D_3R (3403-fold), an electron-withdrawing chloro substituent (**9b**) resulted in increased D_2R and D_3R affinity and greatly reduced D_4R selectivity compared to **9a** (89-fold and 8-fold, respectively). **9a** and **9b** had similar D_4R functional profiles: partial agonists for receptor-mediated cAMP inhibition (**9a**: E_{max} = 13.1 ± 2.2 %, EC_{50} = 29.5 nM [1.5 – 29.3]; **9b**: E_{max} = 32.3 ± 2.5%, EC_{50} = 272 nM [110 – 646]) but antagonists for β-arrestin recruitment (**9a**: I_{max} = 100 ± 6%, IC_{50} = 2340 nM [1370 – 3950]; **9b**: I_{max} = 93.9 ± 5.4%, IC_{50} = 3260 nM [1970 – 5310]. At D_2R and D_3R, **9a** and **9b** exhibited similar partial agonism for cAMP (E_{max} = ~50-54%) but diverged in β-arrestin efficacy where 9a was a partial agonist (**9a**: E_{max} = 37.1 ± 4.8% at D_2R, E_{max} = 60.5 ± 6.3% at D_3R) and **9b** had no

measurable β-arrestin recruitment, suggesting that electron donating/withdrawing groups at this position can substantially alter receptor signaling characteristics.

Comparing the 6-chlorobenzo[*d*]thiazole analogue **9b** to the 5-chlorobenzo[*d*]thiazole analogue **9c** and the 4-chlorobenzo[*d*]thiazole analogue **9d** reveals other marked effects. These variations decreased D_4R binding affinity (K_i = ~11-37 nM) but concomitantly decreased D_2R and D_3R binding affinities as well, resulting in improved D_4R selectivity. **9b** is a D_4R partial agonist at cAMP (E_{max} = 32.3%) but **9c** and **9d** have no detectable D_4R agonist activity and are full antagonists; all are full antagonists for β-arrestin recruitment. At D_2R, **9c** and **9d** exhibited higher partial D_2R agonism for cAMP (E_{max} = ~78-85%) than **9b** (E_{max} = 50.2%) but had little-to-no detectable β-arrestin recruitment. At D_3R, **9b** and **9d** have no detectable β-arrestin recruitment, but the 5-chloro analogue **9c** gains partial agonism (E_{max} = 32.8 ± 7.2%) albeit at very low potency (24,000 nM [9070 – 76,600]). Together, these data indicate that methyl and chloro substituents on the benzo[*d*]thiazole can shift the functional profile at D_4R with a moderate loss of potency. However, the decreased D_4R potency appears to be less sensitive to these substituents than the D_2R and D_3R where affinity and functional potency are nearly ablated.

Replacing the 1-(pyridin-2-yl)piperazine of **9a** with 2-(piperidin-4-yl)pyridine (**10a**) resulted in a slight improvement in binding affinity across all receptors, but D_4R selectivity was generally maintained over D_2R (150-fold) and D_3R (257-fold). This shift resulted in partial agonist efficacy at D_4R-mediated cAMP inhibition (E_{max} = 24.2 ± 2.1%, EC_{50} = 150 nM [42.3 – 593]) but reduced efficacy in D_2R-mediated cAMP inhibition (E_{max} = 27.0 ± 3.1%, EC_{50} = 496 nM [165 – 1500]). In β-arrestin recruitment assays, **10a** was inactive as an agonist for all receptors tested but a full antagonist at the D_4R (I_{max} = 98.6 ± 2.7%, IC_{50} = 248 nM [187 – 237]), D_2R (I_{max} = 92.5 ± 3.8%, IC_{50} = 2780 nM [1980 – 3910]), and D_3R (I_{max} = 97.0 ± 6.3%, IC_{50} = 6700 nM [4330 – 10,400]).

Replacing the methyl group with a methoxy group at the 4 position (**10c**), and then moving the methoxy group to the 3 position (**10b**) improved D_4R binding affinity (K_i = 6.12 ± 4.06 nM, K_i = 21.3 ± 7.6 nM, respectively) compared to **10a**. However, **10b** gained D_2R and D_3R affinity (K_i = 669 ± 354, K_i = 228 ± 82 nM, respectively) while **10c** only gained D_2R binding affinity (K_i = 427 ± 189 nM). **10b** was a cAMP partial agonist at D_4R (E_{max} = 11.3 ± 1.2%, EC_{50} = 12.7 nM [2.6 – 58.1]) and D_2R (E_{max} = 42.4 ± 5.1%, EC_{50} = 183 nM [45.2 – 649]) and it exhibited antagonism for β-arrestin recruitment at all receptors (D_2R, I_{max} = 98.3 ± 3.4%, IC_{50} = 2260 nM [1660 – 3070]; D_3R, I_{max} = 107 ± 6%, IC_{50} = 2770 nM [1820 – 4200]; D_4R, I_{max} = 103 ± 3%, IC_{50} = 122 nM [86.5 – 172]). **10c** was also a partial agonist at the D_4R (E_{max} = 30.5 ± 2.1%, EC_{50} = 38.6 nM [12.8 – 114]) and D_2R (E_{max} = 65.3 ± 5.5%, EC_{50} = 228 nM [102 – 488]) for cAMP inhibition. In notable contrast to **10b**, **10c** exhibited partial β-arrestin recruitment agonism at the D_2R (E_{max} = 29.0 ± 2.0%, EC_{50} = 1170 nM [498 – 2890]) and D_3R (E_{max} = 31.4 ± 2.5%, EC_{50} = 3790 nM [1400 – 9660]) but no agonist activity was detected at the D_4R where it was an antagonist (I_{max} = 93.7 ± 3.0%, IC_{50} = 724 nM [528 – 990]).

Overall, the initial and expanded library included four key classes of modifications with distinct effects on binding and efficacy profiles across the D_2-like receptors. We find the following structure-activity relationships: 1) Reducing the linker chain length from a butyl linker to a propyl linker dramatically improved D_4R binding selectivity over D_2R and D_3R. This is consistent with prior literature[18, 19] that supports alkyl linker length substantially driving D_2-like subtype selectivity. 2) Substitution of the pyrimidine ring in initial lead **5a** with a pyridinyl moiety further improved D_4R binding affinity and selectivity over D_2R and D_3R. 3) Piperazine and piperidine ring moieties produce differential effects on cAMP and β-arrestin signaling at each receptor. 4) Substitutions at different positions on the benzo[*d*]thiazole moiety substantially altered binding

and functional profiles and warrant more detailed follow-up studies. We also note that 5-substituted pyridine rings (**5c**, **5d**, **6b**) were full antagonists, consistent with prior published reports.[2, 20, 21]

5f was one of our first compounds that completed *in vitro* characterization, and was chosen for further analysis based on its pharmacological profile: high D_4R binding affinity with excellent selectivity over D_2R and D_3R (1326-fold and 520-fold, respectively), as measured by [^{3}H]*N*-methylspiperone competition (**Table 1**), and excellent D_4R selectivity in both cAMP and β-arrestin recruitment antagonism (**Table 2** and **Table 3**). **5f** is a low-efficacy D_4R partial agonist, as measured in cAMP inhibition assays (**Figure 2A** and **Table 2**) and a full antagonist in β-arrestin recruitment assays (**Figure 2B** and **Table 3**), maintaining 97-fold D_4R selectivity over D_2R in cAMP antagonist assays, 391-fold D_4R selectivity over D_2R in β-arrestin recruitment antagonist assays, and 859-fold D_4R selectivity over D_3R in β-arrestin recruitment antagonist assays, indicating it is highly subtype-selective. We conducted Schild-type analysis of **5f** using the β-arrestin recruitment assay to determine whether **5f** was a competitive orthosteric antagonist without any allosteric activity. Dopamine concentration-response curves were conducted in the presence of DMSO and increasing concentrations of **5f** (**Figure 2C**). The dopamine curves shifted to the right without decreasing dopamine efficacy, indicating **5f** is a competitive antagonist. Schild-type analysis revealed the slope approached unity (slope = 1.09) and its affinity was 11.0 nM (**Figure 2C inset**). Together these results indicated that **5f** is a potent and selective D_4R antagonist suitable for further analyses.

Compound 5f selectivity at an array of CNS GPCRs and monoamine transporters

Our results indicated that **5f** is highly D_4R-selective compared to the other D_2-like receptors (D_2R and D_3R). In order to determine the selectivity of **5f** at other biogenic amine receptors, **5f**

was tested at the Psychoactive Drug Screening Program (PDSP), which tests compounds at an array of GPCRs and monoamine transporters.[22] In an initial high concentration (10 μM) screen, **5f** displayed greater than 50% radioligand inhibition at 23 GPCRs/transporters. These were further tested in full concentration-response analyses to determine the affinity of **5f** at each receptor/transporter (**Table 4**). Only six GPCRs showed affinity higher than 100 nM: σ2, 5-HT_{1A}, 5-HT_{2A}, 5-HT_{2B}, α2C, and D_4R (**Table 4**). The PDSP-determined affinity of **5f** for the D_4R was 9.48 nM, consistent with the results we obtained (K_i = 2.21 nM). **5f** had comparable affinity for 5-HT_{1A} (5.8 nM), 5-HT_{2B} (13 nM) and lower affinity for 5-HT_{2A} (46 nM), α2C (73 nM), and σ2 (73 nM; **Table 4**). Given the important roles that serotonin receptors can play in substance use disorders, we further characterized the signaling effects of **5f** at the three highest affinity secondary targets, 5-HT_{1A}, 5-HT_{2A}, and 5-HT_{2B}.

To determine its functional activity at 5-HT_{1A}, 5-HT_{2A}, and 5-HT_{2B}, **5f** was tested in $G\alpha_i$ or $G\alpha_q$ calcium flux assays by Eurofins Discovery (Eurofins Cerep SA, Celle l'Evescault, France and Eurofins DiscoverX Corporation, Fremont, CA). The results of these assays are shown in **Table 5**. When tested at 5-HT_{1A} in the $G\alpha_i$ calcium flux assay, **5f** showed agonist activity with an estimated potency of 4.6 μM. The curve did not saturate at the highest tested concentration (10 μM), so the estimated E_{max} (58.8% of the serotonin response) may be an underestimate due to the low apparent potency of **5f** at 5-HT_{1A} for $G\alpha_i$-coupled responses. Because agonist responses interfere with analysis of the antagonist mode of this assay, the IC_{50} of **5f** as >370 nM reflects the highest drug concentration not excluded from analysis. In $G\alpha_q$ calcium flux assays, **5f** had no agonist activity at 5-HT_{2A} or 5-HT_{2B} (EC_{50} > 10 μM), and was a full antagonist at both receptors (5-HT_{2A} I_{max} = 106%, IC_{50} = 532 nM; 5-HT_{2B} I_{max} = 111%, IC_{50} = 770 nM). In comparison, **5f** had higher potency at D_4R, with an IC_{50} of 69.3 nM in cAMP assays that are also responsive to $G\alpha_{i/o}$-

mediated signaling (**Table 2**). While one should be cautious about over-interpreting relative potencies collected across different assay conditions, these results suggest that **5f** is modestly D_4R-selective over 5-HT_{2A} and 5-HT_{2B} with potential low potency agonism at 5-HT_{1A}.

In silico and *in vitro* pharmacokinetics studies of 5f

The potential for brain penetrance of **5f** was evaluated *in silico* using central nervous system multiparameter optimization (CNS MPO) tools. **5f**, and the brain-penetrant CNS ligand buspirone as a comparator, had calculated CNS MPO scores of 4.5 and 5.8, respectively shown in Supplemental **Table S3**; scores >4 correlate with CNS drug-like properties.[23] **5f** was also tested in Caco-2 membrane permeability assays (Eurofins Panlabs, St. Charles, MO) and the apical-to-basolateral (A-B) permeability of **5f** was 27×10^{-6} cm/s, comparable to the assay control compounds propranolol (24×10^{-6} cm/s) and buspirone (25×10^{-6} cm/s), correlate with high membrane permeability.

We then evaluated the Phase I metabolic stability of **5f** using rat and human liver microsomes as previously described.[24] Incubation of **5f** with rat liver microsomes in the presence of NADPH resulted in time-dependent degradation, with ~33% remaining after 1 hour (**Figure 3A**). In human liver microsomes, **5f** showed greater stability, with ~60% remaining after 1 hour incubation (**Figure 3B**). These results predict that **5f** has modest liver metabolic stability in humans and relatively lower stability in rat liver.

Pharmacokinetic assessment of 5f in rats

Given its adequate stability profile, we next evaluated the *in vivo* pharmacokinetic profile of **5f** in rats. Sprague Dawley rats were dosed with **5f** (10 mg/kg, i.p.) and plasma and brain levels of

were measured 0 – 6 hours post-dose. The results from the pharmacokinetic analysis are shown in **Figure 4A-B**. **5f** demonstrated good exposure in both plasma and brain, with $AUC_{0\text{-}t}$ values of 1.05 nmol*h/mL and 3.67 nmol*h/g respectively. Compound **5f** was observed to have a brain penetration index ($AUC_{brain/plasma}$ ratio) of 3.5 with an apparent half-life of ~1 hour ($t_{1/2}$). The detailed pharmacokinetic parameters of the **5f** are provided in **Figure 4B**.

Behavioral effects of 5f in rats trained to self-administer food and cocaine.

In order to test our hypothesis that D_4R antagonism is a viable route for CUD pharmacotherapy, we evaluated whether **5f** altered cocaine self-administration, using food self-administration as natural reward comparator. Separate groups of male Fischer 344 rats were trained to respond on a lever to receive food pellets or i.v. cocaine in multicomponent procedures. Both procedures included 3 components (60 min each for cocaine, 30 min each for food) in each test wherein the reinforcer was reduced across components (food: 4, 2 and 1 food pellets across components 1, 2, and 3, respectively; i.v. cocaine: 166, 83, 41.5 mg/infusion across components 1, 2, and 3, respectively). After successful training, saline vehicle and **5f** (5, 15, and 30 mg/kg, i.p.) were tested.

5f pretreatment produced a significant decrease in the number of infusions for each cocaine dose, an effect that was dependent upon the dose of the compound (5, 15 and 30 mg/kg, i.p.) (**Figure 5A**). Intake following saline pretreatment was not significantly different from baseline [$F_{2, 16} = 0.2935$, $P=0.75$]. A significant main effect of compound **5f** on cocaine self-administration was observed [$F_{1.239, 34.69} = 57.79$, $P<0.0001$] and a significant interaction of component and **5f** on cocaine intake [$F_{6, 56} = 3.181$, $P=0.0093$]. The number of infusions obtained for each cocaine dose

was significantly different after **5f** treatment and the magnitude of effect was dependent on the dose of **5f** as well as the dose of cocaine self-administered.

Similarly, **5f** dose-dependently decreased food maintained responding (**Figure 5B**). Intake following saline pretreatment was not significantly different from baseline [$F_{2, 32}$ = 1.949, P=0.1589]. A significant main effect of **5f** on food-maintained responding was observed [$F_{1.708, 49.53}$ = 137.4, P<0.0001] and a significant interaction of Component and **5f** on cocaine intake [$F_{6, 58}$ = 32.88, P<0.0001].

Overall, these results indicate that **5f** is centrally active and reduces cocaine- and food-maintained responding. The effects of **5f** are most pronounced at lower unit doses of cocaine but at higher unit doses of food, suggesting some differentiation of these effects that will be more fully evaluated in follow-up studies. Future testing will also determine whether **5f** affects relapse-like responding and other behaviors relevant to CUD.

CONCLUSIONS

Evidence from human genetic studies and animal models suggest D_4R signaling modulates drug-taking and -seeking behaviors. Newer highly selective D_4R antagonists will be useful to better characterize the role of D_4R signaling *in vivo*, particularly in behavioral models of CUD. This study provided a detailed structure-activity relationship analysis of a novel series of D_4R partial agonists and antagonists. We identified several compounds with high D_4R binding affinity and selectivity over other D_2-like receptors (D_2R, D_3R) with diverse partial agonist and antagonist profiles. The low-efficacy D_4R partial agonist **5f** was chosen as a lead compound suitable for pharmacokinetic and behavioral testing on the basis of its high selectivity over D_2R and D_3R. **5f**

displayed acceptable *in vitro* metabolic stability in rat and human liver microsomes and good *in vivo* half-life and brain penetration parameters.

In behavioral testing, **5f** dose-dependently decreased cocaine- and food-maintained operant responding, with diverging effects on the reinforcer unit dose. These results suggest that D_4R antagonism reduces the rewarding effects of cocaine and is a plausible route for CUD pharmacotherapy development. We cannot rule out the importance of off-target effects in the behavioral response to **5f**—the compound is only modestly D_4R-selective over its antagonistic effects at 5-HT_{2A} and 5-HT_{2B} receptors. This may actually represent a favorable profile, as prior studies have reported that 5-HT_{2A} and 5-HT_{2B} antagonists can attenuate cocaine-taking and -seeking behaviors.[25-29] Our results also suggest the possibility of **5f** producing low potency agonism at 5-HT_{1A}, which has been previously reported to increase the reinforcing strength of a low cocaine dose.[30] This is at odds with our behavioral results, which seem to indicate a stronger effect of **5f** at lower unit doses of cocaine.

The extended analogue library created while analyzing **5f** *in vitro* and *in vivo* identified several additional modifications that improved D_4R affinity and selectivity over D_2R and D_3R; future analyses will determine whether these modifications alter activity at 5-HT_{2A}, 5-HT_{2B}, and 5-HT_{1A}. We are optimistic that these analogues will be useful as novel *in vivo* research tools and plan to examine additional ADME characteristics of selected library members. It is interesting to speculate that a collection of ligands with varying efficacies may allow for the fine-tuning of D_4R inhibition, potentially leading to a fuller understanding of functional consequences of D_4R signaling levels in development of therapeutics for SUDs and other neuropsychiatric disorders.

EXPERIMENTAL METHODS

Reaction conditions and yields were not optimized. Anhydrous solvents were purchased from Aldrich and were used without further purification. All other chemicals and reagents were purchased from Sigma-Aldrich Co. LLC, Aurora Fine Chemicals LLC, VWR Chemicals, Enamine, Acros Organics, and Alfa Aesar. All amine final products were converted into either the oxalate or hydrochloride salt. Spectroscopic data and yields refer to the free base form of compounds. Flash chromatography was performed using silica gel (EMD Chemicals, Inc.; 230-400 mesh, 60 Å) by using Teledyne ISCO CombiFlash RF system. ^{1}H and ^{13}C spectra were acquired using a JEOL ECZ-400S NMR spectrometer. ^{1}H chemical shifts are reported as parts per million (δ ppm) relative to tetramethylsilane (0.00 ppm). All the coupling constants are measured in Hz. Chemical shifts for ^{13}C NMR spectra are reported as parts per million (δ ppm) and referenced according to deuterated solvent for ^{1}H spectra ($CDCl_3$, 7.26 or CD_3OD, 3.31) and ^{13}C spectra ($CDCl_3$, 77.1 or CD_3OD, 49.0). Chemical shifts, multiplicities, and coupling constants (J) have been reported and calculated using MNova 64. Combustion analysis was performed by Atlantic Microlab, Inc. (Norcross, GA) and the results agree within ± 0.4% of calculated values (**Table S1**). cLogP and PSA values were calculated using ChemDraw version 20.0. Melting point determination was conducted using a SRS OptiMelt MPA100-Automated melting point apparatus and are uncorrected. Based on NMR and combustion analysis data, all final compounds are ≥95% pure. All compounds within this series are covered under an existing patent,[14] but only **5a** and **5e**[13] have been previously described in the peer-reviewed literature.

General Method A.[13] 4-chlorobutanoyl chloride or 5-chloropentanoyl chloride (1.24 equiv) was added dropwise to a solution of substituted or unsubstituted 2-aminobenzenethiol (1.00 equiv) in toluene at 0 °C over 15 minutes, an off-white precipitate was formed. The reaction mixture was stirred at room temperature for 48 hrs, under N_2 atmosphere. After the reaction was complete, the

solvent was removed *in vacuo.* The crude mixture was diluted with aqueous $NaHCO_3$ (100 mL) and EtOAc (100 mL), the two layers were separated and then extracted with EtOAc (2 × 100 mL) and washed with brine (100 mL). The combined organic layer was dried over Na_2SO4, filtered and concentrated. The product was purified by flash column chromatography (5-95% EtOAc:Hexanes) gradient to give the desired substituted or unsubstituted 2-(3-chloropropyl)benzo[*d*]thiazole or 2-(4-chlorobutyl)benzo[*d*]thiazole compounds.

*2-(4-chlorobutyl)benzo[d]thiazole **(4a)***.[13] The compound **4a** was synthesized as described for general method **A** by using 5-chloropentanoyl chloride (5.87 g, 49.5 mmol), 2-aminobenzenethiol (4.27 mL, 39.9 mmol) in toluene (150 mL). The product **4a** is formed as brown sticky oil (5.98 g, 66% yield). ^{1}H NMR (CD_3OD) δ 8.26 (d, *J* = 8.1 Hz, 1H), 8.16 (d, *J* = 8.5 Hz, 1H), 7.94 – 7.84 (m, 1H), 7.80 (t, *J* = 7.7 Hz, 1H), 4.83 – 4.81 (m, 2H), 4.62 (t, *J* = 6.1 Hz, 2H), 2.38 – 2.27 (m, 2H), 2.20 – 2.10 (m, 2H).

*2-(3-chloropropyl)benzo[d]thiazole **(4b)**.*[13] The compound **4b** was synthesized as described for general method **A** by using 4-chlorobutanoyl chloride (5.54 mL, 49.53 mmol), 2-aminobenzenethiol (4.27 mL, 39.9 mmol) in toluene (150 mL). The product **4b** formed as greenish oil (6.30 g, 75% yield). ^{1}H NMR ($CDCl_3$) δ 7.96 (dd, *J* = 8.0, 1.5 Hz, 1H), 7.83 (dt, *J* = 8.5, 1.2 Hz, 1H), 7.44 (ddq, *J* = 8.2, 7.1, 1.1 Hz, 1H), 7.34 (ddt, *J* = 8.2, 7.1, 1.0 Hz, 1H), 3.66 (td, *J* = 6.2, 1.0 Hz, 2H), 3.27 (td, *J* = 7.3, 1.2 Hz, 2H), 2.41 – 2.30 (m, 2H).

*2-(3-chloropropyl)-6-methylbenzo[d]thiazole **(8a)***. The compound **8a** was synthesized as described for general method **A** by using 4-chlorobutanoyl chloride (1.00 mL, 8.91 mmol), 2-amino-5-methylbenzenethiol (1.00 g, 7.18 mmol) in toluene (50 mL). The product **8a** formed as yellowish oil (1.39 g, 86% yield). ^{1}H NMR ($CDCl_3$) δ 7.86 (s, 1H), 7.83 (d, *J* = 8.2 Hz, 1H), 7.60

(d, *J* = 14.5 Hz, 1H), 3.66 (td, *J* = 6.0, 1.7 Hz, 2H), 3.31 – 3.03 (m, 2H), 2.51 (d, *J* = 38.0 Hz, 3H), 2.40 – 2.22 (m, 2H).

2-(3-chloropropyl)-7-methoxybenzo[d]thiazole ***(8b).*** The compound **8b** was synthesized as described for general method **A** by using 4-chlorobutanoyl chloride (0.89 mL, 7.98 mmol), 2-amino-6-methoxybenzenethiol (1.00 g, 6.44 mmol) in toluene (100 mL). The product **8b** formed as black solid (1.05 g, 67% yield). ^{1}H NMR ($CDCl_3$) δ 7.59 (dt, *J* = 8.1, 0.8 Hz, 1H), 7.39 (td, *J* = 8.0, 0.7 Hz, 1H), 6.80 (d, *J* = 8.0 Hz, 1H), 3.97 (s, 3H), 3.66 (t, *J* = 6.4 Hz, 2H), 3.28 (t, *J* = 7.3 Hz, 2H), 2.43 – 2.30 (m, 2H).

2-(3-chloropropyl)-6-methoxybenzo[d]thiazole ***(8c).*** The compound **8c** was synthesized as described for general method **A** by using 4-chlorobutanoyl chloride (0.89 mL, 7.99 mmol), 2-amino-5-methoxybenzenethiol (1.00 g, 6.44 mmol) in toluene (50 mL). The product **8c** is formed as dark brown solid (890 mg, 57% yield). ^{1}H NMR (CD_3OD) δ 7.94 (d, *J* = 9.1 Hz, 1H), 7.87 – 7.69 (m, 1H), 7.18 – 6.98 (m, 1H), 4.83 (s, 3H), 3.76 – 3.59 (m, 2H), 3.33 – 3.18 (m, 2H), 2.91 (p, *J* = 7.7 Hz, 2H).

6-chloro-2-(3-chloropropyl)benzo[d]thiazole ***(8d).*** The compound **8d** was synthesized as described for general method **A** by using 4-chlorobutanoyl chloride (0.87 mL, 7.77 mmol), 2-amino-5-chlorobenzenethiol (1.00 g, 6.26 mmol) in toluene (50 mL). The product **8d** is formed as brown solid (1.13 g, 73% yield). ^{1}H NMR ($CDCl_3$) δ 7.89 – 7.80 (m, 2H), 7.43 – 7.40 (m, 1H), 3.67 (t, *J* = 6.3 Hz, 2H), 3.27 (t, *J* = 7.4 Hz, 2H), 2.42 – 2.31 (m, 2H).

5-chloro-2-(3-chloropropyl)benzo[d]thiazole ***(8e).*** The compound **8e** was synthesized as described for general method **A** by using 4-chlorobutanoyl chloride (1.74 mL, 15.5 mmol), 2-amino-4-chlorobenzenethiol (2.00 g, 12.5 mmol) in toluene (75 mL). The product **8e** is formed as

yellowish solid (1.73 g, 56% yield). ^{1}H NMR ($CDCl_3$) δ 7.95 (d, *J* = 2.0 Hz, 1H), 7.74 (d, *J* = 8.5 Hz, 1H), 7.34 (dd, *J* = 8.5, 2.0 Hz, 1H), 3.67 (t, *J* = 6.3 Hz, 2H), 3.28 (t, *J* = 7.4 Hz, 2H), 2.36 (tt, *J* = 7.5, 6.3 Hz, 2H).

4-chloro-2-(3-chloropropyl)benzo[d]thiazole ***(8f).*** The compound **8f** was synthesized as described for general method A by using 4-chlorobutanoyl chloride (1.74 mL, 15.5 mmol), 2-amino-3-chlorobenzenethiol (2.00 g, 12.5 mmol) in toluene (100 mL). The product **8f** is formed as black solid (1.85 g, 60% yield). ^{1}H NMR ($CDCl_3$) δ 7.89 – 7.78 (m, 1H), 7.44 – 7.38 (m, 1H), 7.25 (dd, *J* = 2.9, 1.8 Hz, 1H), 3.67 (t, *J* = 6.3 Hz, 2H), 3.33 – 3.21 (m, 2H), 2.43 – 2.29 (m, 2H).

General Method B. Substituted or unsubstituted 2-(3-chloropropyl)benzo[*d*]thiazole or 2-(4-chlorobutyl)benzo[*d*]thiazole (1.0 equiv) was added to a solution of K_2CO_3 (10 equiv), KI (0.1 equiv), substituted or unsubstituted arylpiperidinyl or arylpiperazinyl (1.2 equiv) in an anhydrous acetonitrile solution. The reaction mixture was stirred at reflux (80 °C) for 20 hrs, under N_2 atmosphere. The reaction mixture was cooled to room temperature and the solvent was removed *in vacuo*. The residue was diluted with water (100 mL) and dichloromethane (DCM) (100 mL), and then extracted with DCM (3 x 100 mL) and washed with brine (100 mL). The combined organic layer was dried over Na_2SO4, filtered, and then evaporated to afford crude products. All final products were purified by flash column chromatography eluting with 5% CMA, (95% chloroform, 4% methanol, 1% ammonium hydroxide) gradient to give the desired compounds.

2-(4-(4-(pyrimidin-2-yl)piperazin-1-yl)butyl)benzo[d]thiazole ***(5a)***. Compound **5a** was synthesized as described for general method B by using K_2CO_3 (4.28 g, 31.0 mmol), KI (52 mg), 2-(4-chlorobutyl)benzo[*d*]thiazole **(4a)** (700 mg, 3.10 mmol), 2-(piperazin-1-yl)pyrimidine (0.53 mL, 3.72 mmol) in an anhydrous acetonitrile (18 mL) solution. The crude product was purified by

flash column chromatography to obtain pure **5a** as a cream solid (320 mg, 29% yield). ^{1}H NMR (400 MHz $CDCl_3$) δ 8.26 (d, *J* = 4.8 Hz, 2H), 7.93 (d, *J* = 8.0 Hz, 1H), 7.80 (d, *J* = 7.6 Hz, 1H), 7.43 – 7.39 (m, 1H), 7.33 – 7.29 (m, 1H), 6.44 – 6.41 (m, 1H), 3.80 – 3.78 (m, 4H), 3.13 (t, *J* = 7.6 Hz, 2H), 2.46 – 2.38 (m, 6H), 1.92 (p, *J* = 7.2 Hz, 2H), 1.65 (p, *J* = 7.6 Hz, 2H). ^{13}C NMR (101 MHz, $CDCl_3$) δ 171.85, 161.61, 157.66, 153.20, 135.09, 125.88, 124.67, 122.50, 121.47, 109.76, 58.19, 53.09, 43.63, 34.12, 27.55, 26.27. The HCl salt was precipitated from 2-propanol. Mp 239-241 °C. Anal. ($C_{19}H_{23}N_5S$•2HCl•0.5H_2O) C, H, N.

*2-(4-(4-(pyridin-2-yl)piperazin-1-yl)butyl)benzo[d]thiazole **(5b)***. Compound **5b** was synthesized as described for general method B by using K_2CO_3 (4.28 g, 31.0 mmol), KI (52 mg), 2-(4-chlorobutyl)benzo[*d*]thiazole **(4a)** (700 mg, 3.10 mmol), 1-(pyridin-2-yl)piperazine (0.57 mL, 3.72 mmol) in an anhydrous acetonitrile (18 mL) solution. The crude product was purified by flash column chromatography to obtain pure **5b** as a cream solid (313 mg, 29% yield). ^{1}H NMR (400 MHz $CDCl_3$) δ 8.18 – 8.17 (m, 1H), 7.97 – 7.94 (m, 1H), 7.84 – 7.82 (m, 1H), 7.47 – 7.42 (m, 2H), 7.36 – 7.34 (m, 1H), 6.63 – 6.58 (m, 2H), 3.54 – 3.51 (m, 4H), 3.16 (t, *J* = 7.6 Hz, 2H), 2.54 (t, *J* = 4.8 Hz, 4H), 2.45 – 2.42 (m, 2H), 1.92 (p, *J* = 8.0 Hz, 2H), 1.68 (p, *J* = 7.6 Hz, 2H). ^{13}C NMR (101 MHz, $CDCl_3$) δ 171.90, 159.54, 153.22, 147.94, 137.41, 135.11, 125.91, 124.69, 122.52, 121.50, 113.24, 107.02, 58.21, 53.08, 45.18, 34.15, 27.60, 26.31. The HCl salt was precipitated from 2-propanol. Mp 235-237 °C. Anal. ($C_{20}H_{24}N_4S$•3HCl•1.5H_2O) C, H, N.

*2-(4-(4-(5-methylpyridin-2-yl)piperazin-1-yl)butyl)benzo[d]thiazole **(5c)***. Compound **5c** was synthesized as described for general method B by using K_2CO_3 (1.96 g, 14.2 mmol), KI (24 mg), 2-(4-chlorobutyl)benzo[*d*]thiazole **(4a)** (320 mg, 1.42 mmol), 1-(5-methylpyridin-2-yl)piperazine (302 mg, 1.70 mmol) in an anhydrous acetonitrile (8 mL) solution. The crude product was purified by flash column chromatography to obtain pure **5c** as a light brown solid (153 mg, 31% yield). ^{1}H

NMR (400 MHz $CDCl_3$) δ 8.01 (s, 1H), 7.96 (d, *J* = 7.2 Hz, 1H), 7.85 – 7.983 (m, 1H), 7.45 – 7.43 (m, 1H), 7.36 – 7.29 (m, 2H), 6.57 (d, *J* = 8.4 Hz, 1H), 3.48 (t, *J* = 5.2 Hz, 4H), 3.17 (t, *J* = 7.6 Hz, 2H), 2.55 (t, *J* = 5.2 Hz, 4H), 2.46 – 2.42 (m, 2H), 2.19 (s, 3H), 1.94 (p, *J* = 7.6 Hz, 2H), 1.65 (p, *J* = 8.0 Hz, 2H). ^{13}C NMR (101 MHz, $CDCl_3$) δ 171.92, 158.14, 153.22, 147.66, 138.35, 135.12, 125.90, 124.68, 122.52, 122.29, 121.50, 106.97, 58.24, 53.09, 45.69, 34.16, 27.62, 26.33, 17.33. The HCl salt was precipitated from 2-propanol. Mp 200-202 °C. Anal. ($C_{21}H_{26}N_4S$•3HCl•1.25H_2O) C, H, N.

2-(4-(4-(5-chloropyridin-2-yl)piperazin-1-yl)butyl)benzo[d]thiazole ***(5d)***. Compound **5d** was synthesized as described for general method B by using K_2CO_3 (3.06 g, 22.2 mmol), KI (37 mg), 2-(4-chlorobutyl)benzo[*d*]thiazole **(4a)** (500 mg, 2.22 mmol), 1-(5-chloropyridin-2-yl)piperazine (525 mg, 2.66 mmol) in an anhydrous acetonitrile (13 mL) solution. The crude product was purified by flash column chromatography to obtain pure **5d** as a white solid **(**202 mg, 24% yield). ^{1}H NMR (400 MHz $CDCl_3$) δ 8.09 (q, *J* = 2.4 Hz, 1H), 7.99 – 7.91 (m, 1H), 7.86 – 7.79 (m, 1H), 7.49 – 7.31 (m, 3H), 6.56 (dt, *J* = 9.2, 2.3 Hz, 1H), 3.50 (q, *J* = 4.4 Hz, 4H), 3.19 – 3.11 (m, 2H), 2.56 – 2.49 (m, 4H), 22.39 (m, 2H), 1.92 (q, *J* = 7.9 Hz, 2H), 1.72 – 1.60 (m, 2H). ^{13}C NMR (101 MHz, $CDCl_3$) δ 171.96, 157.91, 153.33, 146.33, 137.18, 135.21, 126.03, 124.81, 122.62, 121.60, 120.22, 107.83, 58.22, 52.98, 45.37, 34.22, 31.03, 27.64. The Oxalate salt was precipitated from 2-propanol/acetone. Mp 214-215 °C. Anal. ($C_{20}H_{23}ClN_4S$•$C_2H_2O_4$) C, H, N.

2-(3-(4-(pyrimidin-2-yl)piperazin-1-yl)propyl)benzo[d]thiazole ***(5e)***. The compound **5e** was synthesized as described for general method **B** by using K_2CO_3 (4.66 g, 33.7 mmol), KI (60 mg), 2-(3-chloropropyl)benzo[*d*]thiazole **(4b)** (714 mg, 3.37 mmol), 2-(piperazin-1-yl)pyrimidine (0.57 mL, 4.04 mmol) in an anhydrous acetonitrile (20 mL) solution. The crude product was purified by flash column chromatography to obtain pure **5e** as a brown oil (480 mg, 42% yield). ^{1}H NMR (400

MHz $CDCl_3$) δ 8.27 (d, *J* = 4.8 Hz, 2H), 7.96 (d, *J* = 8.4 Hz, 1H), 7.82 – 7.80 (m, 1H), 7.44 – 7.39 (m, 1H), 7.34 – 7.29 (m, 1H), 6.45 – 6.42 (t, *J* = 4.8 Hz, 1H), 3.81 – 3.79 (m, 4H), 3.17 (t, *J* = 7.6 Hz, 2H), 2.49 – 2.46 (m, 6H), 2.11 (p, *J* = 7.2 Hz, 2H). ^{13}C NMR (101 MHz, $CDCl_3$) δ 171.68, 161.60, 157.67, 153.21, 135.13, 125.89, 124.69, 122.50, 121.48, 109.77, 57.44, 53.01, 43.64, 32.08, 26.68. The HCl salt was precipitated from 2-propanol. Mp 182-184 °C. Anal. ($C_{18}H_{21}N_5S$•2HCl•1.75H_2O) C, H, N.

*2-(3-(4-(pyridin-2-yl)piperazin-1-yl)propyl)benzo[d]thiazole **(5f)***. Compound **5f** was synthesized as described for general method B by using K_2CO_3 (4.56 g, 33.0 mmol), KI (55 mg), 2-(3-chloropropyl)benzo[*d*]thiazole **(4b)** (700 mg, 3.30 mmol), 1-(pyridin-2-yl)piperazine (0.53 mL, 3.72 mmol) in an anhydrous acetonitrile (20 mL) solution. The crude product was purified by flash column chromatography to obtain pure **5f** as a brown oil (530 mg, 47% yield). ^{1}H NMR (400 MHz $CDCl_3$) δ 8.18 – 8.16 (m, 1H), 7.96 (d, *J* = 7.2 Hz, 1H), 7.83 – 7.81 (m, 1H), 7.46 – 7.41 (m, 2H), 7.35 – 7.31 (m, 1H), 6.62 – 6.57 (m, 2H), 3.54 – 3.51 (m, 4H), 3.18 (t, *J* = 7.2 Hz, 2H), 2.56 – 2.48 (m, 6H), 2.11 (p, *J* = 7.6 Hz, 2H). ^{13}C NMR (101 MHz, $CDCl_3$) δ 171.70, 159.52, 153.23, 147.94, 137.42, 135.16, 125.91, 124.70, 122.51, 121.49, 113.24, 107.02, 57.43, 52.97, 45.19, 32.09, 26.73. The HCl salt was precipitated from 2-propanol. Mp 245-247 °C. Anal. ($C_{19}H_{22}N_4S$•3HCl•2H_2O) C, H, N.

*2-(3-(4-(4-methylpyridin-2-yl)piperazin-1-yl)propyl)benzo[d]thiazole **(5g)***. Compound **5g** was synthesized as described for general method B by using K_2CO_3 (4.89 g, 35.4 mmol), KI (59 mg), 2-(3-chloropropyl)benzo[*d*]thiazole **(4b)** (750 mg, 3.54 mmol), 1-(4-methylpyridin-2-yl)piperazine (754 mg, 4.25 mmol) in an anhydrous acetonitrile (21 mL) solution. The crude product was purified by flash column chromatography to obtain pure **5g** as a brown oil (360 mg, 29% yield). ^{1}H NMR (400 MHz $CDCl_3$) δ 8.04 (d, *J* = 4.9 Hz, 1H), 7.96 (d, *J* = 8.1 Hz, 1H), 7.86

– 7.81 (m, 1H), 7.46– 7.82 (m, 1H), 7.34 (td, *J* = 7.6, 1.2 Hz, 1H), 6.46 (d, *J* = 5.9 Hz, 2H), 3.53 (t, *J* = 5.1 Hz, 4H), 3.18 (t, *J* = 7.6 Hz, 2H), 2.61 – 2.48 (m, 6H), 2.25 (s, 3H), 2.13 (p, *J* = 7.5 Hz, 2H).). ^{13}C NMR (101 MHz, $CDCl_3$) δ 171.73, 159.89, 153.33, 148.51, 147.67, 135.27, 126.02, 124.82, 122.63, 121.60, 115.03, 107.65, 57.53, 53.06, 45.46, 32.18, 26.69, 21.53. The HCl salt was precipitated from 2-propanol. Mp 213-215 °C. Anal. ($C_{20}H_{24}N_4S$•3HCl•1.75H_2O) C, H, N.

2-(3-(4-(3-methoxypyridin-2-yl)piperazin-1-yl)propyl)benzo[d]thiazole ***(5h)***. Compound **5h** was synthesized as described for general method B by using K_2CO_3 (4.89 g, 35.4 mmol), KI (41 mg), 2-(3-chloropropyl)benzo[*d*]thiazole **(4b)** (523 mg, 2.47 mmol), 1-(3-methoxypyridin-2-yl)piperazine (570 mg, 2.97 mmol) in an anhydrous acetonitrile (15 mL) solution. The crude product was purified by flash column chromatography to obtain pure **5h** as a brown oil (380 mg, 42% yield). ^{1}H NMR (400 MHz $CDCl_3$) δ 7.98 – 7.92 (m, 1H), 7.88 – 7.80 (m, 2H), 7.46– 7.42 (m, 1H), 7.36– 7.32 (m, 1H), 7.01 (dd, *J* = 8.0, 1.5 Hz, 1H), 6.82 (dd, *J* = 7.9, 4.9 Hz, 1H), 3.83 (s, 3H), 3.45 (s, 4H), 3.18 (t, *J* = 7.5 Hz, 2H), 2.62 (d, *J* = 40.6 Hz, 6H), 2.08 – 2.05 (m, 2H). ^{13}C NMR (101 MHz, $CDCl_3$) δ 146.87, 138.96, 135.28, 126.04, 124.88, 122.64, 121.63, 117.57, 74.55, 55.36, 34.21, 31.83, 29.62, 29.30, 25.41, 25.36, 22.67, 14.16. The HCl salt was precipitated from 2-propanol. Mp 154-156 °C. Anal. ($C_{20}H_{24}N_4OS$•3HCl•1.5H_2O) C, H, N.

2-(3-(4-(3-methylpyridin-2-yl)piperidin-1-yl)propyl)benzo[d]thiazole ***(6a)***. Compound **6a** was synthesized as described for general method B by using K_2CO_3 (3.66 g, 26.5 mmol), KI (44 mg), 2-(3-chloropropyl)benzo[*d*]thiazole **(4b)** (561 mg, 2.65 mmol), 3-methyl-2-(piperidin-4-yl)pyridine (560 mg, 3.18 mmol) in an anhydrous acetonitrile (16 mL) solution. The crude product was purified by flash column chromatography to obtain pure **6a** as a brown oil (680 mg, 73% yield). ^{1}H NMR (400 MHz $CDCl_3$) δ 8.38 (dd, *J* = 4.8, 1.7 Hz, 1H), 7.95 (dt, *J* = 8.1, 0.9 Hz, 1H), 7.85 – 7.79 (m, 1H), 7.42 (ddd, *J* = 8.2, 7.2, 1.3 Hz, 1H), 7.38 – 7.29 (m, 2H), 6.98 (dd, *J* = 7.6,

4.7 Hz, 1H), 3.17 (t, *J* = 7.6 Hz, 2H), 3.06 (dd, *J* = 10.6, 3.1 Hz, 2H), 2.82 (tt, *J* = 10.9, 3.6 Hz, 1H), 2.48 (t, *J* = 7.2 Hz, 2H), 2.30 (s, 3H), 2.12 – 2.03 (m, 4H), 1.75 – 1.67 (m, 2H), 1.31 – 1.22 (m, 2H). ^{13}C NMR (101 MHz, $CDCl_3$) δ 172.26, 162.81, 153.35, 146.91, 137.75, 135.35, 130.28, 125.92, 124.70, 122.56, 121.60, 121.06, 57.55, 54.25, 40.52, 32.10, 30.91, 27.07, 18.73. The Oxalate salt was precipitated from 2-propanol. Mp 167-168 °C. Anal. ($C_{21}H_{25}N_3S$•$C_2H_2O_4$•0.25H_2O•0.75C_3H_7OH) C, H, N.

2-(3-(4-(5-methoxypyridin-2-yl)piperidin-1-yl)propyl)benzo[d]thiazole ***(6b)***. Compound **6b** was synthesized as described for general method B by using K_2CO_3 (7.19 g, 52.0 mmol), KI (86 mg), 2-(3-chloropropyl)benzo[*d*]thiazole **(4b)** (1.10 g, 5.20 mmol), 5-methoxy-2-(piperidin-4-yl)pyridine (1.00 g, 6.24 mmol) in an anhydrous acetonitrile (30 mL) solution. The crude product was purified by flash column chromatography to obtain pure **6b** as stick brown oil (880 mg, 46% yield). ^{1}H NMR (400 MHz $CDCl_3$) δ 8.20 (d, *J* = 2.9 Hz, 1H), 7.97 – 7.92 (m, 1H), 7.85 – 7.80 (m, 1H), 7.43 (ddd, *J* = 8.3, 7.2, 1.3 Hz, 1H), 7.33 (ddd, *J* = 8.2, 7.2, 1.2 Hz, 1H), 7.13 (dd, *J* = 8.7, 2.9 Hz, 1H), 7.07 (d, *J* = 8.6 Hz, 1H), 3.81 (s, 3H), 3.16 (t, *J* = 7.5 Hz, 2H), 3.06 (dt, *J* = 11.8, 3.2 Hz, 2H), 2.66 (tt, *J* = 11.7, 3.9 Hz, 1H), 2.51 (dd, *J* = 8.4, 6.3 Hz, 2H), 2.11 (td, *J* = 9.5, 3.2 Hz, 4H), 1.99 – 1.87 (m, 2H), 1.79 (qd, *J* = 12.3, 3.7 Hz, 2H). ^{13}C NMR (101 MHz, $CDCl_3$) δ 171.97, 157.21, 154.08, 153.34, 136.41, 135.32, 125.97, 124.76, 122.61, 121.59, 121.43, 120.71, 57.74, 55.70, 54.08, 43.62, 32.29, 28.72, 26.94. The Oxalate salt was precipitated from 2-propanol. Mp 181-182 °C. Anal. ($C_{21}H_{25}N_3OS$•$C_2H_2O_4$) C, H, N.

6-methyl-2-(3-(4-(pyridin-2-yl)piperazin-1-yl)propyl)benzo[d]thiazole ***(9a)***. Compound **9a** was synthesized as described for general method B by using K_2CO_3 (4.28 g, 31.1 mmol), KI (52 mg), 2-(3-chloropropyl)-6-methylbenzo[*d*]thiazole **(8a)** (700 mg, 3.10 mmol), 1-(pyridin-2-yl)piperazine (607 mg, 3.72 mmol) in an anhydrous acetonitrile (18 mL) solution. The crude

product was purified by flash column chromatography to obtain pure **9a** as a light brown solid (460 mg, 42% yield). ^{1}H NMR (400 MHz $CDCl_3$) δ 8.17 (ddd, *J* = 4.9, 2.0, 0.9 Hz, 1H), 7.82 (d, *J* = 8.3 Hz, 1H), 7.61 (s, 1H), 7.45 (ddd, *J* = 8.9, 7.1, 1.9 Hz, 1H), 7.23 (d, *J* = 1.7 Hz, 1H), 6.67 – 6.56 (m, 2H), 3.53 (t, *J* = 5.1 Hz, 4H), 3.14 (t, *J* = 7.6 Hz, 2H), 2.56 (t, *J* = 5.1 Hz, 4H), 2.50 (dd, *J* = 8.4, 6.3 Hz, 2H), 2.45 (s, 3H), 2.10 (p, *J* = 7.5 Hz, 2H). ^{13}C NMR (101 MHz, $CDCl_3$) δ 170.67, 159.62, 151.40, 148.04, 137.56, 135.40, 134.86, 127.55, 122.08, 121.38, 113.38, 107.16, 57.56, 53.06, 45.26, 32.13, 26.79, 21.56. The HCl salt was precipitated from 2-propanol. Mp 230-231 °C. Anal. ($C_{20}H_{24}N_4S$•3HCl•$2H_2O$) C, H, N.

*6-chloro-2-(3-(4-(pyridin-2-yl)piperazin-1-yl)propyl)benzo[d]thiazole **(9b)***. Compound **9b** was synthesized as described for general method **B** by using K_2CO_3 (5.05 g, 36.6 mmol), KI (61 mg), 6-chloro-2-(3-chloropropyl)benzo[*d*]thiazole **(8d)** (900 mg, 3.66 mmol), 1-(pyridin-2-yl)piperazine (716 mg, 4.39 mmol) in an anhydrous acetonitrile (22 mL) solution. The crude product was purified by flash column chromatography to obtain pure **9b** as a brown solid (510 mg, 38% yield). ^{1}H NMR (400 MHz $CDCl_3$) δ 8.17 (dd, *J* = 4.9, 2.1 Hz, 1H), 7.88 – 7.78 (m, 2H), 7.49 – 7.38 (m, 2H), 6.65 – 6.58 (m, 2H), 3.53 (t, *J* = 5.1 Hz, 4H), 3.17 (t, *J* = 7.5 Hz, 2H), 2.62 – 2.47 (m, 6H), 2.15 – 2.05 (m, 2H). ^{13}C NMR (101 MHz, $CDCl_3$) δ 172.36, 159.61, 151.90, 148.06, 137.56, 136.47, 130.73, 126.80, 123.35, 121.23, 113.41, 107.16, 57.43, 53.05, 45.27, 32.15, 26.62. The HCl salt was precipitated from 2-propanol. Mp 233-235 °C. Anal. ($C_{19}H_{21}ClN_4S_3$•3HCl•$0.5H_2O$) C, H, N.

*5-chloro-2-(3-(4-(pyridin-2-yl)piperazin-1-yl)propyl)benzo[d]thiazole **(9c)***. Compound **9c** was synthesized as described for general method **B** by using K_2CO_3 (5.61 g, 40.6 mmol), KI (67 mg), 5-chloro-2-(3-chloropropyl)benzo[*d*]thiazole **(8e)** (1.00 g, 4.06 mmol), 1-(pyridin-2-yl)piperazine (796 mg, 4.88 mmol) in an anhydrous acetonitrile (24 mL) solution. The crude product was

purified by flash column chromatography to obtain pure **9c** as a light brown solid (650 mg, 43% yield). ^{1}H NMR (400 MHz $CDCl_3$) δ 8.21 – 8.13 (m, 1H), 7.93 (d, *J* = 2.1 Hz, 1H), 7.73 (d, *J* = 8.5 Hz, 1H), 7.49 – 7.41 (m, 1H), 7.31 (dd, *J* = 8.6, 2.1 Hz, 1H), 6.66 – 6.57 (m, 2H), 3.53 (t, *J* = 5.0 Hz, 4H), 3.17 (t, *J* = 7.5 Hz, 2H), 2.62 – 2.45 (m, 6H), 2.11 (p, *J* = 7.4 Hz, 2H). ^{13}C NMR (101 MHz, $CDCl_3$) δ 173.84, 159.61, 154.23, 148.05, 137.55, 133.53, 132.05, 125.31, 122.54, 122.28, 113.41, 107.16, 57.43, 53.05, 45.27, 32.24, 26.65. The HCl salt was precipitated from 2-propanol. Mp 239-241 °C. Anal. ($C_{19}H_{21}ClN_4S$•3HCl•1.75H_2O) C, H, N.

4-chloro-2-(3-(4-(pyridin-2-yl)piperazin-1-yl)propyl)benzo[d]thiazole ***(9d)***. Compound **9d** was synthesized as described for general method **B** by using K_2CO_3 (5.61 g, 40.6 mmol), KI (67 mg), 4-chloro-2-(3-chloropropyl)benzo[*d*]thiazole **(8f)** (1.00 g, 4.06 mmol), 1-(pyridin-2-yl)piperazine (796 mg, 4.88 mmol) in an anhydrous acetonitrile (24 mL) solution. The crude product was purified by flash column chromatography to obtain pure **9d** as a cream solid (830 mg, 55% yield). ^{1}H NMR (400 MHz $CDCl_3$) δ 8.17 (ddd, *J* = 4.9, 2.1, 1.0 Hz, 1H), 7.88 – 7.78 (m, 2H), 7.49 – 7.37 (m, 2H), 6.62 (ddt, *J* = 8.4, 7.2, 2.9 Hz, 2H), 3.54 (t, *J* = 5.0 Hz, 4H), 3.17 (t, *J* = 7.5 Hz, 2H), 2.55 (dt, *J* = 24.6, 6.2 Hz, 6H), 2.12 (p, *J* = 7.3 Hz, 2H). ^{13}C NMR (101 MHz, $CDCl_3$) δ 172.15, 159.48, 151.89, 148.06, 137.61, 136.47, 130.76, 126.82, 123.36, 121.24, 113.52, 107.19, 57.38, 52.95, 45.10, 32.08, 26.36. The HCl salt was precipitated from 2-propanol. Mp 233-234 °C. Anal. ($C_{19}H_{21}ClN_4S$•3HCl•0.25H_2O) C, H, N.

6-methyl-2-(3-(4-(pyridin-2-yl)piperidin-1-yl)propyl)benzo[d]thiazole ***(10a)***. Compound **10a** was synthesized as described for general method B by using K_2CO_3 (4.10 g, 29.7 mmol), KI (49 mg), 2-(3-chloropropyl)-6-methylbenzo[*d*]thiazole **(8a)** (670 mg, 2.97 mmol), 2-(piperidin-4-yl)pyridine (574 mg, 3.56 mmol) in an anhydrous acetonitrile (18 mL) solution. The crude product was purified by flash column chromatography to obtain pure **10a** as a sticky brown oil (630 mg,

60% yield). ^{1}H NMR (400 MHz $CDCl_3$) δ 8.50 (ddd, *J* = 5.0, 1.9, 0.9 Hz, 1H), 7.82 (d, *J* = 8.3 Hz, 1H), 7.62 – 7.57 (m, 2H), 7.23 (d, *J* = 1.7 Hz, 1H), 7.14 (dd, *J* = 7.9, 1.2 Hz, 1H), 7.09 (ddd, *J* = 7.4, 4.8, 1.1 Hz, 1H), 3.13 (t, *J* = 7.6 Hz, 2H), 3.06 (dt, *J* = 11.7, 3.0 Hz, 2H), 2.69 (tt, *J* = 12.1, 3.9 Hz, 1H), 2.48 (dd, *J* = 8.5, 6.3 Hz, 2H), 2.45 (s, 3H), 2.14 – 2.03 (m, *J* = 7.1, 4.6 Hz, 4H), 1.99 – 1.89 (m, 2H), 1.80 (qd, *J* = 12.3, 3.7 Hz, 2H). ^{13}C NMR (101 MHz, $CDCl_3$) δ 170.94, 165.14, 151.41, 149.18, 136.61, 135.45, 134.78, 127.50, 122.06, 121.41, 121.38, 120.70, 57.79, 54.09, 44.70, 32.26, 32.08, 27.06, 21.56. The oxalate salt was precipitated from 2-propanol. Mp 151-152 °C. Anal. ($C_{21}H_{25}N_3S•2C_2H_2O_4$) C, H, N.

7-methoxy-2-(3-(4-(pyridin-2-yl)piperidin-1-yl)propyl)benzo[d]thiazole ***(10b)***. Compound **10b** was synthesized as described for general method B by using K_2CO_3 (2.57 g, 18.6 mmol), KI (31 mg), 2-(3-chloropropyl)-7-methoxybenzo[*d*]thiazole **(8b)** (450 mg, 1.86 mmol), 2-(piperidin-4-yl)pyridine (330 mg, 2.05 mmol) in an anhydrous acetonitrile (11 mL) solution. The crude product was purified by flash column chromatography to obtain pure **10b** as a brown oil (443 mg, 65% yield). ^{1}H NMR (400 MHz $CDCl_3$) δ 8.51 (ddd, *J* = 4.9, 1.9, 1.0 Hz, 1H), 7.64 – 7.56 (m, 2H), 7.38 (t, *J* = 8.1 Hz, 1H), 7.15 (dt, *J* = 8.0, 1.1 Hz, 1H), 7.09 (ddd, *J* = 7.5, 4.9, 1.1 Hz, 1H), 6.82 – 6.76 (m, 1H), 3.96 (s, 3H), 3.16 (t, *J* = 7.6 Hz, 2H), 3.06 (dt, *J* = 11.9, 3.1 Hz, 2H), 2.69 (tt, *J* = 12.0, 3.9 Hz, 1H), 2.49 (dd, *J* = 8.4, 6.3 Hz, 2H), 2.10 (qd, *J* = 8.7, 6.5 Hz, 4H), 1.98 – 1.90 (m, 2H), 1.81 (qd, *J* = 12.3, 3.8 Hz, 2H). ^{13}C NMR (101 MHz, $CDCl_3$) δ 172.55, 165.18, 155.03, 154.30, 149.18, 136.57, 126.85, 123.85, 121.37, 120.69, 115.31, 104.85, 57.74, 55.96, 54.09, 44.71, 32.29, 32.09, 27.13. The oxalate salt was precipitated from 2-propanol. Mp 174-175 °C. Anal. ($C_{21}H_{25}N_3OS•C_2H_2O_4$) C, H, N.

6-methoxy-2-(3-(4-(pyridin-2-yl)piperidin-1-yl)propyl)benzo[d]thiazole ***(10c)***. Compound **10c** was synthesized as described for general method B by using K_2CO_3 (2.34 g, 16.9 mmol), KI (28

mg), 2-(3-chloropropyl)-6-methoxybenzo[*d*]thiazole **(8c)** (409 mg, 1.69 mmol), 2-(piperidin-4-yl)pyridine (300 mg, 1.86 mmol) in an anhydrous acetonitrile (10 mL) solution. The crude product was purified by flash column chromatography to obtain pure **10c** as a dark brown oil (300 mg, 48% yield). ^{1}H NMR (400 MHz $CDCl_3$) δ 8.51 (ddd, *J* = 4.9, 1.9, 1.0 Hz, 1H), 7.82 (d, *J* = 8.9 Hz, 1H), 7.60 (td, *J* = 7.7, 1.8 Hz, 1H), 7.29 (d, *J* = 2.6 Hz, 1H), 7.15 (d, *J* = 7.9 Hz, 1H), 7.09 (ddd, *J* = 7.5, 4.8, 1.2 Hz, 1H), 7.03 (dd, *J* = 8.9, 2.5 Hz, 1H), 3.85 (s, 3H), 3.15 – 3.02 (m, 4H), 2.69 (tt, *J* = 12.1, 3.9 Hz, 1H), 2.49 (t, *J* = 7.3 Hz, 2H), 2.09 (td, *J* = 11.2, 5.0 Hz, 4H), 1.94 (d, *J* = 13.5 Hz, 2H), 1.88 – 1.69 (m, 2H). ^{13}C NMR (101 MHz, $CDCl_3$) δ 169.07, 164.73, 157.45, 149.19, 147.76, 136.70, 136.53, 123.02, 121.47, 120.77, 115.14, 104.28, 57.58, 55.93, 55.89, 55.85, 53.86, 44.27, 32.04, 31.58, 26.55. The HCl salt was precipitated from 2-propanol. Mp 170-171 °C. Anal. ($C_{21}H_{25}N_3OS•C_2H_2O_4$) C, H, N.

Radioligand binding assays.

Binding at dopamine D_2-like receptors was determined similarly to previously described methods.[2, 31] Membranes were prepared from HEK293 cells stably expressing human $D_{2L}R$, D_3R, or D_4R grown in a 50:50 mix of DMEM and Ham's F12 culture media, supplemented with 20 mM HEPES, 2 mM L-glutamine, 0.1 mM non-essential amino acids, 1X antibiotic/antimycotic, 10% heat-inactivated fetal bovine serum, and 200 µg/mL hygromycin (Life Technologies, Grand Island, NY) and kept in an incubator at 37 °C and 5% CO_2. Upon reaching 80-90% confluence, cells were harvested using pre-mixed Earle's Balanced Salt Solution (EBSS) with 5 mM EDTA (Life Technologies) and centrifuged at 3,000 rpm for 10 min at 21 °C. The supernatant was removed, and the pellet was resuspended in 10 mL hypotonic lysis buffer (5 mM $MgCl_2 \cdot 6\ H_2O$, 5 mM Tris, pH 7.4 at 4 °C) and centrifuged at 14,500 rpm (~25,000 g) for 30 min at 4 °C. The pellet was then resuspended in fresh EBSS binding buffer made from 8.7 g/L Earle's Balanced Salts without

phenol red (US Biological, Salem, MA), 2.2 g/L sodium bicarbonate, pH to 7.4. A Bradford protein assay (Bio-Rad, Hercules, CA) was used to determine the protein concentration and membranes were diluted to 500 µg/mL and stored in a -80 °C freezer for later use.

Radioligand competition binding experiments were conducted using thawed membranes on test day, each test compound was diluted into 10 half-log serial dilutions using 30% DMSO vehicle, starting from 1 mM or 100 µM concentration. Previously frozen membranes were diluted in fresh EBSS binding buffer to 200 µg/mL (for $hD_{2L}R$ or hD_3R) or 400 µg/mL (for hD_4R) for binding. Radioligand competition experiments were conducted in 96-well plates containing 300 µl fresh EBSS binding buffer, 50 µl of diluted test compound, 100 µl of membranes (20 µg/well total protein for $hD_{2L}R$ and hD_3R, and 50 µl of [^{3}H]*N*-methylspiperone radioligand diluted in binding buffer (0.4 nM final concentration; Perkin Elmer). Nonspecific binding was determined using 10 µM (+)-butaclamol (Sigma-Aldrich, St. Louis, MO) and total binding was determined with 30% DMSO vehicle. All compound dilutions were tested in triplicate and the reaction incubated for 1 hour at RT. The reaction was terminated by filtration through Perkin Elmer Uni-Filter-96 GF/C plates, presoaked for 1 hour in 0.5% polyethylenimine, using a Brandel 96-Well Plates Harvester Manifold (Brandel Instruments, Gaithersburg, MD). The filters were washed (3 × 1 mL/well) of ice-cold binding buffer. Perkin Elmer MicroScint 20 Scintillation Cocktail (65 µL) was added to each well and filters were counted using a Perkin Elmer MicroBeta Microplate Counter. IC_{50} values for each compound were determined from dose-response curves and K_i values were calculated using the Cheng-Prusoff equation.[47] When a complete inhibition couldn't be achieved at the highest tested concentrations, K_i values have been extrapolated by constraining the bottom of the dose-response curves (= 0% residual specific binding) in the non-linear regression analysis. These analyses were performed using GraphPad Prism versions 6.00-8.00 (GraphPad Software,

San Diego, CA). All results were rounded to three significant figures. K_i values were determined from at least 3 independent experiments and are reported as means ± SEM.

Functional Assays.

cAMP Inhibition Assay

D_4R and D_2R -mediated inhibition of forskolin-stimulated cAMP production was assayed using the PerkinElmer LANCE UltracAMP assay kit (PerkinElmer, Inc., Waltham, MA). CHO-K1 cells stably expressing the human D_2R long isoform or D_4R were maintained in Ham's F12 supplemented with 10% fetal bovine serum, 100 U/ml penicillin, 100 µg/ml streptomycin, 800 µg/ml G418 and 300 µg/ml hygromycin at 37°C, 5% CO_2, and 90% humidity. Cells were seeded in 5 µl Hank's Balanced Salt Solution (with CaCl and $MgCl_2$) with 5mM HEPES buffer and 0.2 µM sodium metabisulfite at a density of 5000 cells/well in 384-well white plates. Compounds and forskolin were made in the same buffer. Immediately after plating, cells were treated with 2.5 µl of compound (at various concentrations) and 2.5 µl of forskolin and incubated at room temperature for 30 minutes. The final concentration of forskolin was 10 µM. When running the assay in antagonist mode, the EC_{80} of dopamine (10 nM) was added with the Forskolin solution. Eu-cAMP tracer and ULight-anti-cAMP solutions were added as directed by the manufacturer and cells were incubated for 2 hours in the dark at room temperature, after which a TR-FRET signal was measured using a BMG Labtech PHERAstar FS (BMG Labtech, NC). Values were normalized to a percentage of the control TR-FRET signal seen with a maximum concentration of dopamine for agonist mode assays and the EC_{80} of dopamine for antagonist mode assays. Data was collected in triplicate from at least three independent experiments. Data analysis and normalization was performed in GraphPad Prism 9 (GraphPad Software, CA). First, raw data was fit using a log(agonist/antagonist) vs. response – Variable slope (four parameters) curve fit. The data were

normalized to the percent maximum dopamine response (agonist mode) or the EC_{80} of dopamine (antagonist mode). The Hill coefficients of the concentration-response curves did not significantly differ from unity with the data fitting to a single site model. Graphs are meaned concentration response curves from at least three independent experiments. Data in **Table 2** was extracted from the meaned curves where E_{max}/I_{max} are expressed as mean ± SEM and the potencies are expressed as mean [95% confidence interval]. Fold selectivity for the D_4R over the D_2R were also calculated and presented in **Table 2**.

β-Arrestin Recruitment Assay

Assays were conducted with minor modifications as previously published by our laboratory[2, 19-23] using the DiscoverX PathHunter technology (Eurofins DiscoverX, Fremont, CA). Briefly, CHO-K1 cells stably expressing the human D_2R long isoform, D_3R, or D_4R (Eurofins DiscoverX) were maintained in Ham's F12 media supplemented with 10% fetal bovine serum, 100 U/mL penicillin, 100 μg/ml streptomycin, 800 μg/ml G418 and 300 μg/ml hygromycin at 37 °C, 5% CO_2, and 90% humidity. The cells were seeded in 7.5 μl media at a density of 2,625 cells/well in 384-well black, clear-bottom plates. The following day, the compounds were diluted in PBS with 0.2 μM sodium metabisulfite. The cells were treated with 16 concentrations of a compound in triplicate and incubated at 37 °C for 90 minutes. Tropix Gal-Screen Substrate (Applied Biosystems, MA) was diluted in Gal-Screen buffer A (Applied Biosystems) 1:25 and added to cells according to the manufacturer's recommendations followed by a 30–45-minute incubation at room temperature in the dark. Luminescence was measured on a Hamamatsu FDSS μCell reader. Data was collected in triplicate and transferred to GraphPad Prism 9 where it was fit with a log(agonist/antagonist) vs. response – Variable slope (four parameters) curve fit. The data were normalized to the percent

maximum dopamine response (agonist mode) or the EC_{80} of dopamine (antagonist mode). The Hill coefficients of the concentration-response curves did not significantly differ from unity with the data fitting to a single site model. Graphs are meaned concentration response curves from at least three independent experiments. Data in **Table 3** was extracted from the meaned curves where E_{max}/I_{max} are expressed as mean ± SEM and the potencies are expressed as mean [95% confidence interval]. Fold selectivity for the D_4R over the D_2R and D_3R were also calculated and presented in **Table 3**.

Schild-type analysis – β-Arrestin Recruitment Assay

Schild-type analysis using the β-arrestin recruitment assay is conducted similarly except for compound preparation. Compounds were diluted in PBS with 0.2 μM sodium metabisulfite at eight concentrations ranging from 10 μM to 10 nM (final in assay concentrations) and a DMSO control. The compounds were added to the cells followed immediately by a dopamine concentration response curve and returned to the incubator at 37 °C for 90 minutes. The Tropic Gal-Screen substrate and buffer were prepared and added as previously described. All other aspects of the Schild-type analysis were identical to the β-arrestin recruitment assay procedure. Data was collected in triplicate and transferred to GraphPad Prism 9 (GraphPad Software, CA) where it was fit with a log(agonist) vs. response – Variable slope (four parameters) curve fit. The data was normalized to the maximum dopamine/DMSO response. Graphs are meaned concentration response curves from at least three independent experiments. Schild-type plots were generated by plotting the log scale compound concentration (x-axis) versus the log((A'/A)-1) where A' is the EC_{50} of the dopamine curve obtained for each concentration of antagonist and A is the EC_{50} of

dopamine in the DMSO control. Simple linear regression was performed in GraphPad Prism 9 were the slope and x-intercept indicate competitiveness and the affinity of compound, respectively.

Rat and human microsomal stability assays

Phase I metabolic stability assays were conducted using rat and human liver microsomes as previously described[24, 32] with minor modifications. In brief, the reactions were carried out with 100 mM potassium phosphate buffer, pH 7.4, in the presence of NADPH regenerating system (1.3 mM NADPH, 3.3 mM glucose 6-phosphate, 3.3 mM $MgCl_2$, 0.4 U/mL glucose-6-phosphate dehydrogenase, 50 µM sodium citrate). Negative controls without cofactors were assessed to determine the non-CYP mediated metabolism. Positive controls for phase I metabolism (Buprenorphine) were also evaluated. Compound disappearance was monitored over time using a liquid chromatography and tandem mass spectrometry (LC/MS) method. All reactions were performed in triplicate.

Chromatographic analysis was performed on a Dionex ultra high-performance LC system coupled with Q Exactive Focus orbitrap mass spectrometer (Thermo Fisher Scientific Inc., Waltham MA). Separation was achieved using Agilent Eclipse Plus column (100 × 2.1mm i.d; maintained at 35 °C) packed with a 1.8 µm C18 stationary phase. The mobile phase used was composed of 0.1% Formic Acid in Acetonitrile and 0.1% Formic Acid in water with gradient elution, starting with 2.5% organic phase (from 0 to 2 min) linearly increasing to 99% (from 2 to 5.5 min), and re-equilibrating to 2.5% by 6.5 min. The total run time for each analyte was 6.5 min. Pumps were operated at a flow rate of 0.3 mL/min. The mass spectrometer controlled by Xcalibur software 4.0.27.13 (Thermo Scientific) was operated with a HESI ion source in positive ionization mode. Compounds were identified in the full-scan mode (from *m/z* 50 to 750) by comparing t = 0 samples with t = 30 min and t = 60 min samples.

Pharmacokinetics study in rats

Pharmacokinetic studies in Sprague Dawley (SD) rats were conducted according to protocols approved by the Animal Care and Use Committee at Johns Hopkins University. SD rats obtained from Harlan were maintained on a 12 h light−dark cycle with ad libitum access to food and water. Test compound was administered via i.p. injection at a dose of 10 mg/kg (100% saline vehicle, 10 ml/kg volume). The rats were sacrificed at specified time points (0.25, 0.5 h, 1, 2, 4, and 6 h) post drug administration. For the collection of plasma and brain tissue, animals were euthanized with CO_2, and blood samples were collected in heparinized microtubes by cardiac puncture. Brains were dissected and immediately flash-frozen (−80 °C). Blood samples were spun at 2000 g for 15 min, and plasma was removed and stored at −80 °C until analysis (as described below).

Bioanalysis. Quantitation of **5f** was performed using liquid chromatography with tandem mass spectrometry (LC/MS-MS) methods. Briefly, calibration standards were prepared using respective tissue (naïve plasma and brain) with additions of the test compound. For quantifying the test compound in the pharmacokinetic samples, plasma samples (20 μL) were processed using a single liquid extraction method by addition of 100 μL of acetonitrile containing internal standard (losartan: 0.5 μM), followed by vortex-mixing for 30 s and then centrifugation at 10,000 × g for 10 min at 4 °C. Brain tissues were diluted 1:5 w/v with acetonitrile containing losartan (0.5 μm) and homogenized, followed by vortex-mixing and centrifugation at 10,000 × g for 10 min at 4 °C. A 50 μL aliquot of the supernatant was diluted with 50 μL of water and transferred to 250 μL polypropylene autosampler vials sealed with teflon caps. 2 μL of the sample was injected into the LC/MS/MS system for analysis. Chromatographic analysis was performed using an Accela ultra high-performance system consisting of an analytical pump and an autosampler coupled with a TSQ Vantage mass spectrometer. Separation of analyte was achieved at ambient temperature using

Agilent Eclipse Plus column (100 × 2.1 mm i.d.) packed with a 1.8 μm C18 stationary phase. The mobile phase consisted of 0.1% formic acid in acetonitrile and 0.1% formic acid in water with gradient elution, starting with 10% organic phase (from 0 to 1 min) linearly increasing to 95% (from 1 to 2 min), and re-equilibrating to 10% by 3 min. The total run time for each analyte was 3.5 min. Pumps were operated at a flow rate of 0.3 mL/min. The $[M+H]^+$ ion transition of test compound (CAB-01-019) (m/z 339.1638 → 121.0759, 176.0528) and losartan (IS) (m/z 423.1695 → 192.0808, 207.0914) were used. Plasma concentrations (nmol/ml) as well as brain tissue concentrations (nmol/g) were determined and plots of mean plasma concentration versus time were constructed. Non-compartmental analysis modules in Phoenix WinNonlin version 7.0 (Certara USA, Inc., Princeton, NJ) were used to quantify exposures (AUC_{0-t}) and half-life ($t_{1/2}$).

Operant conditioning experiments

Animals: Male Fischer 344 rats (100-130 days; Charles River, Wilmington, MA) were housed in a temperature-controlled vivarium on a 12-hour reversed light/dark cycle (lights on at 6:00 PM). Rats were group-housed two per cage with water available *ad libitum* while food access was restricted to maintain consistent body weight during the experiment. Experimental sessions were conducted during the dark phase of the light/dark cycle. All procedures were performed in accordance with the High Point University Institutional Animal Care and Use Committee and the National Institutes of Health Guide for the Care and Use of Laboratory Animals (NIH Publication No. 80-23) revised in 1996.

Food maintained responding. For experiments, rats were transferred to operant conditioning chambers (ENV-008CT; Med-Associates, St. Albans, VT) enclosed in sound-attenuating cubicles (ENV-018; Med Associates). The front panel of the operant chambers contained two response

levers (4 cm above the floor and 3 cm from each side wall), a cue light (3 cm above each of the two levers) and a food chute centered on the front wall (2 cm above the floor) that was connected to a food pellet dispenser (ENV-023; Med Associates) located behind the front wall and a tone generator to mask extraneous noise. Food maintained responding was assessed using a multi-component procedure consisting of three 30-min components separated by 4-min blackout periods between components. Responding was engendered and maintained by delivery of food pellets (45 mg; Noyes, Lancaster, NH; 4, 2 and 1 pellets for Components 1, 2 and 3, respectively) under an FR3 schedule of reinforcement. Completion of the response requirement on the active lever extinguished lights, retracted both levers, delivered food, and was followed by 20 sec time-out (TO) period. After the TO, the lights were illuminated, levers extended, and the FR schedule was in effect. The presentation of **5f** doses (5, 15, 20 and 30 mg/kg, i.p.) and saline were randomly assigned and administered 15 minutes before the start of the session. The criterion for stable responding was two consecutive sessions in which the total number of reinforcers did not vary by more than 10% from baseline levels.

Cocaine self-administration

The operant apparatus has been described above. For self-administration studies, a counterbalance arm was connected at the rear corner of the operant chamber onto which a single channel swivel was mounted. The rat's leash was attached to the swivel and the catheter tubing connected to the bottom port of the swivel. A motor-driven 20 ml syringe pump (PHM-100; Med Associates) was attached outside of the sound-attenuating chamber and polyethylene tubing connected the needle on the syringe to the entry port of the swivel. A PC was used for session programming and data collection (Med Associates Inc., East Fairfield, VT). For lever training, subjects were transferred to the operant chambers for daily experimental sessions and responding was engendered and

maintained by delivery of food pellets (45 mg pellets; Noyes, Lancaster, NH) under an FR1 schedule of reinforcement that was gradually increased to FR3. The lever light was illuminated when the schedule was in effect. Completion of the response requirement on the active lever extinguished lights, retracted both levers, delivered food, and was followed by a 20-second timeout (TO) period during which all lights were off. After the TO, the lights were illuminated, and the FR schedule was in effect. Sessions lasted 30 minutes or until 50 food pellets were delivered. The criterion for stable responding was five consecutive sessions in which the total number of reinforcers did not vary by more than 20% from control levels. Responses on the inactive lever were recorded but had no scheduled consequences.

Intravenous jugular surgery. After operant responding was acquired and maintained by food, subjects were surgically implanted with a venous catheter inserted into the right jugular vein following administration of ketamine (90 mg/kg; i.p.) and xylazine (5 mg/kg; i.p.) for anesthesia as described previously.[33-35] Catheters were anchored to muscle near the point of entry into the vein. The distal end of the catheter was guided subcutaneously to exit above the scapulae through a Teflon shoulder harness. The harness provided a point of attachment for a spring leash connected to a single-channel fluid swivel at the opposing end. The catheter was threaded through the leash and attached to the swivel. The other end of the swivel was connected to a syringe (for saline and drug delivery) mounted on a syringe pump. Rats were administered penicillin G procaine (75,000 units in 0.25 mL, i.m.) and allowed a minimum of 5 days to recover before self-administration studies were initiated. Following surgery, rats received hourly infusions of heparinized 0.9% bacteriostatic saline (1.7 U/ml; 200 μl/hour) using a computer-controlled motor-driven syringe pump in the home cage vivarium. The health of the rats was monitored daily by the experimenters and weekly by an institutional veterinarian per the guidelines issued by the High Point University

Institutional Animal Care and Use Committee and the National Institutes of Health. Infusions of propofol (6 mg/kg; i.v.) were administered to assess catheter patency, as needed.

Responding was maintained under an FR3: 20-sec TO of three 1-hr components. Subjects were allowed to self-administer cocaine i.v. (166, 83, 41.5 mg/infusion). Each dose was available during a different component, and doses were presented in descending order. The infusion volume for the first component was 400 μl infused over 12 sec, and the volumes for the successive components were 200 μl for component two (infused over 6 sec) and 100 μl for component three (infused over 3 sec). Before each component, a 10-min blackout was followed by a priming infusion of the dose to be administered in the succeeding component. After an additional 10-min blackout period, the lever was activated, and the cue light above the lever was illuminated. The start of each session was indicated by the illumination of the house light, stimulus light above the active lever and the extension of both levers. Upon completion of the response requirement, a drug infusion was delivered, the lever light extinguished, a tone was generated, and the house light was illuminated. During the 20-s TO after the infusion, responses on the lever were recorded but had no scheduled consequence. A minimum of three days of stable responding (less than 10% variation in the number of infusions) at FR3 in all components was required before administration of compounds was initiated.

Effects of 5f on cocaine self-administration: Rats were transferred to the operant chambers for the self-administration sessions. Before each session, the swivel and catheter were flushed with 500 μl of heparinized saline before connecting the catheter to the syringe via a 20 ga Leur hub and 28 ga male connector. Completion of the response requirement on the active lever extinguished

lights, retracted both levers, delivered food, and was followed by 20 sec TO. After the TO, lights were illuminated, levers extended, and the FR schedule was in effect.[33-37]

After a minimum of five days of stable responding (defined as consecutive sessions in which the total number of infusions did not vary by more than 20% from the mean of previous sessions), saline vehicle and **5f** (5, 15, 20, and 30 mg/kg, i.p.) were tested. Dose order was randomly assigned for each subject. **5f** and saline were administered 15 min before the first component.

ASSOCIATED CONTENT

Supporting Information. Elemental analysis for all final compounds results. Molecular docking analysis, CNS-MPO value, SMILES data (CSV). The supporting information is available free of charge on the ACS website.

AUTHOR INFORMATION

Corresponding Authors

*Phone: (336) 841-9718. Fax: (336) 888-6354. E-mail: cboateng@highpoint.edu

*Phone: (856) 256-5422. E-mail: keckt@rowan.edu

ORCID

Comfort A. Boateng: 0000-0003-1907-431X

Thomas M. Keck: 0000-0003-1845-9373

R. Benjamin Free: 0000-0002-2428-0487

Amy H. Newman: 0000-0001-9065-4072

Alessandro Bonifazi: 0000-0002-7306-0114

Scott E. Hemby: 0000-0002-6987-1133

David R. Sibley: 0000-0002-0624-962X

Kent D. Stewart: 0000-0001-6417-6927

Author Contributions

[#]C.A.B. and A.N.N. are equally contributing authors.

Notes

The authors declare no competing financial interest.

ACKNOWLEDGEMENT

Support for this research was provided by High Point University, Fred Wilson School of Pharmacy, NIH NIDA R21DA050896 and American Association of Colleges of Pharmacy New Investigator Award grants. Additional support was provided by the National Institute of Neurological Disorders and Stroke-Intramural Research Program (ZIA-NS002263), National Institute on Drug Abuse-Intramural Research Program (Z1A DA000609), and Rowan University. National Science Foundation Major Research Instrumentation Program (CHE-1919685) for the NMR spectrometer. Research reported in this publication was supported by the National Institute of General Medical Sciences of the National Institutes of Health under Award Number T34GM136492. The content is solely the responsibility of the authors and does not necessarily represent the official views of the National Institutes of Health. Receptor binding profiles and agonist functional data was generously provided by the National Institute of Mental Health's Psychoactive Drug Screening Program, Contract no. HHSN-271-2018-00023-C (NIMH PDSP).

The NIMH PDSP is directed by Bryan L. Roth at the University of North Carolina at Chapel Hill and Project Officer Jamie Driscoll at NIMH, Bethesda MD, USA.

ABBREVIATIONS USED

$CDCl_3$, deuterated chloroform; CD_3OD, deuterated methanol; CMA, chloroform/methanol/ammonium hydroxide; 5% CMA, (95% chloroform, 4% methanol, 1% ammonium hydroxide); EtOAc, Ethyl acetate; DA, dopamine; D_2R, dopamine D_2 receptor; D_3R, dopamine D_3 receptor; D_4R, dopamine D_4 receptor; NMR, nuclear magnetic resonance; RT, room temperature; SAR, structure activity relationship.

REFERENCES

1. Beaulieu, J. M.; Gainetdinov, R. R. The physiology, signaling, and pharmacology of dopamine receptors. *Pharmacol. Rev.* **2011,** *63*, 182-217.

2. Keck, T. M.; Free, R. B.; Day, M. M.; Brown, S. L.; Maddaluna, M. S.; Fountain, G.; Cooper, C.; Fallon, B.; Holmes, M.; Stang, C. T.; Burkhardt, R.; Bonifazi, A.; Ellenberger, M. P.; Newman, A. H.; Sibley, D. R.; Wu, C.; Boateng, C. A. Dopamine D4 Receptor-Selective Compounds Reveal Structure-Activity Relationships that Engender Agonist Efficacy. *J. Med. Chem.* **2019,** *62*, 3722-3740.

3. Giorgioni, G.; Del Bello, F.; Pavletic, P.; Quaglia, W.; Botticelli, L.; Cifani, C.; Micioni Di Bonaventura, E.; Micioni Di Bonaventura, M. V.; Piergentili, A. Recent findings leading to the discovery of selective dopamine D4 receptor ligands for the treatment of widespread diseases. *Eur. J. Med. Chem.* **2021,** *212*, 113141.

4. Lindsley, C. W.; Hopkins, C. R. Return of D4 Dopamine Receptor Antagonists in Drug Discovery. *J. Med. Chem.* **2017,** *60*, 7233-7243.

5. Tomlinson, A.; Grayson, B.; Marsh, S.; Hayward, A.; Marshall, K. M.; Neill, J. C. Putative therapeutic targets for symptom subtypes of adult ADHD: D4 receptor agonism and COMT inhibition improve attention and response inhibition in a novel translational animal model. *Eur Neuropsychopharmacol* **2015,** *25*, 454-467.

6. Rondou, P.; Haegeman, G.; Van Craenenbroeck, K. The dopamine D4 receptor: biochemical and signalling properties. *Cell Mol. Life Sci.* **2010,** *67*, 1971-1986.

7. Di Ciano, P.; Grandy, D. K.; Le Foll, B. Dopamine D4 receptors in psychostimulant addiction. *Adv. Pharmacol.* **2014,** *69*, 301-321.

8. Bergman, J.; Rheingold, C. G. Dopamine D(4) Receptor Antagonists for the Treatment of Cocaine Use Disorders. *CNS Neurol. Disord. Drug Targets* **2015,** *14*, 707-715.

9. Belliotti, T. R.; Wustrow, D. J.; Brink, W. A.; Zoski, K. T.; Shih, Y. H.; Whetzel, S. Z.; Georgic, L. M.; Corbin, A. E.; Akunne, H. C.; Heffner, T. G.; Pugsley, T. A.; Wise, L. D. A series of 6- and 7-piperazinyl- and -piperidinylmethylbenzoxazinones with dopamine D4 antagonist activity: discovery of a potential atypical antipsychotic agent. *J. Med. Chem.* **1999,** *42*, 5181-5187.

10. Patel, S.; Freedman, S.; Chapman, K. L.; Emms, F.; Fletcher, A. E.; Knowles, M.; Marwood, R.; McAllister, G.; Myers, J.; Curtis, N.; Kulagowski, J. J.; Leeson, P. D.; Ridgill, M.; Graham,

M.; Matheson, S.; Rathbone, D.; Watt, A. P.; Bristow, L. J.; Rupniak, N. M.; Baskin, E.; Lynch, J. J.; Ragan, C. I. Biological profile of L-745,870, a selective antagonist with high affinity for the dopamine D4 receptor. *J. Pharmacol. Exp. Ther.* **1997,** *283*, 636-647.

11. Bristow, L. J.; Collinson, N.; Cook, G. P.; Curtis, N.; Freedman, S. B.; Kulagowski, J. J.; Leeson, P. D.; Patel, S.; Ragan, C. I.; Ridgill, M.; Saywell, K. L.; Tricklebank, M. D. L-745,870, a subtype selective dopamine D4 receptor antagonist, does not exhibit a neuroleptic-like profile in rodent behavioral tests. *J. Pharmacol. Exp. Ther.* **1997,** *283*, 1256-1263.

12. Bristow, L. J.; Kramer, M. S.; Kulagowski, J.; Patel, S.; Ragan, C. I.; Seabrook, G. R. Schizophrenia and L-745,870, a novel dopamine D4 receptor antagonist. *Trends Pharmacol. Sci.* **1997,** *18*, 186-188.

13. Sampson, D.; Zhu, X. Y.; Eyunni, S. V.; Etukala, J. R.; Ofori, E.; Bricker, B.; Lamango, N. S.; Setola, V.; Roth, B. L.; Ablordeppey, S. Y. Identification of a new selective dopamine D4 receptor ligand. *Bioorg. Med. Chem.* **2014,** *22*, 3105-3114.

14. Cowart, M. D. L., S.P.; Nelson, S.L.; Stewart, A.O. Fused Bicyclic Aromatic Compounds that are Useful in Treating Sexual Dysfunction. U.S Patent 2006/0172995, . August 3, 2006.

15. Wang, S.; Wacker, D.; Levit, A.; Che, T.; Betz, R. M.; McCorvy, J. D.; Venkatakrishnan, A. J.; Huang, X. P.; Dror, R. O.; Shoichet, B. K.; Roth, B. L. D4 dopamine receptor high-resolution structures enable the discovery of selective agonists. *Science* **2017,** *358*, 381-386.

16. Sastry, G. M.; Adzhigirey, M.; Day, T.; Annabhimoju, R.; Sherman, W. Protein and ligand preparation: parameters, protocols, and influence on virtual screening enrichments. *J. Comput. Aided Mol. Des.* **2013,** *27*, 221-234.

17. Harder, E.; Damm, W.; Maple, J.; Wu, C.; Reboul, M.; Xiang, J. Y.; Wang, L.; Lupyan, D.; Dahlgren, M. K.; Knight, J. L.; Kaus, J. W.; Cerutti, D. S.; Krilov, G.; Jorgensen, W. L.; Abel, R.; Friesner, R. A. OPLS3: A Force Field Providing Broad Coverage of Drug-like Small Molecules and Proteins. *J. Chem. Theory Comput.* **2016,** *12*, 281-296.

18. Banala, A. K.; Levy, B. A.; Khatri, S. S.; Furman, C. A.; Roof, R. A.; Mishra, Y.; Griffin, S. A.; Sibley, D. R.; Luedtke, R. R.; Newman, A. H. N-(3-fluoro-4-(4-(2-methoxy or 2,3-dichlorophenyl)piperazine-1-yl)butyl)arylcarboxamides as selective dopamine D3 receptor ligands: critical role of the carboxamide linker for D3 receptor selectivity. *J. Med. Chem.* **2011,** *54*, 3581-3594.

19. Cha, M. Y.; Choi, B. C.; Kang, K. H.; Pae, A. N.; Choi, K. I.; Cho, Y. S.; Koh, H. Y.; Lee, H. Y.; Jung, D.; Kong, J. Y. Design and synthesis of a piperazinylalkylisoxazole library for subtype selective dopamine receptor ligands. *Bioorg. Med. Chem. Lett.* **2002,** *12*, 1327-1330.

20. Stewart, A. O.; Cowart, M. D.; Moreland, R. B.; Latshaw, S. P.; Matulenko, M. A.; Bhatia, P. A.; Wang, X.; Daanen, J. F.; Nelson, S. L.; Terranova, M. A.; Namovic, M. T.; Donnelly-Roberts, D. L.; Miller, L. N.; Nakane, M.; Sullivan, J. P.; Brioni, J. D. Dopamine D4 ligands and models of receptor activation: 2-(4-pyridin-2-ylpiperazin-1-ylmethyl)-1H-benzimidazole and

related heteroarylmethylarylpiperazines exhibit a substituent effect responsible for additional efficacy tuning. *J. Med. Chem.* **2004,** *47*, 2348-2355.

21. Lober, S.; Hubner, H.; Utz, W.; Gmeiner, P. Rationally based efficacy tuning of selective dopamine d4 receptor ligands leading to the complete antagonist 2-[4-(4-chlorophenyl)piperazin-1-ylmethyl]pyrazolo[1,5-a]pyridine (FAUC 213). *J. Med. Chem.* **2001,** *44*, 2691-2694.

22. Besnard, J.; Ruda, G. F.; Setola, V.; Abecassis, K.; Rodriguiz, R. M.; Huang, X. P.; Norval, S.; Sassano, M. F.; Shin, A. I.; Webster, L. A.; Simeons, F. R.; Stojanovski, L.; Prat, A.; Seidah, N. G.; Constam, D. B.; Bickerton, G. R.; Read, K. D.; Wetsel, W. C.; Gilbert, I. H.; Roth, B. L.; Hopkins, A. L. Automated design of ligands to polypharmacological profiles. *Nature* **2012,** *492*, 215-220.

23. Wager, T. T.; Hou, X.; Verhoest, P. R.; Villalobos, A. Central Nervous System Multiparameter Optimization Desirability: Application in Drug Discovery. *ACS Chem. Neurosci.* **2016,** *7*, 767-775.

24. Battiti, F. O.; Cemaj, S. L.; Guerrero, A. M.; Shaik, A. B.; Lam, J.; Rais, R.; Slusher, B. S.; Deschamps, J. R.; Imler, G. H.; Newman, A. H.; Bonifazi, A. The Significance of Chirality in Drug Design and Synthesis of Bitopic Ligands as D3 Receptor (D3R) Selective Agonists. *J. Med. Chem.* **2019,** *62*, 6287-6314.

25. Sholler, D. J.; Stutz, S. J.; Fox, R. G.; Boone, E. L.; Wang, Q.; Rice, K. C.; Moeller, F. G.; Anastasio, N. C.; Cunningham, K. A. The 5-HT(2A) Receptor (5-HT(2A)R) Regulates Impulsive

Action and Cocaine Cue Reactivity in Male Sprague-Dawley Rats. *J. Pharmacol. Exp. Ther.* **2019,** *368*, 41-49.

26. Pockros, L. A.; Pentkowski, N. S.; Swinford, S. E.; Neisewander, J. L. Blockade of 5-HT2A receptors in the medial prefrontal cortex attenuates reinstatement of cue-elicited cocaine-seeking behavior in rats. *Psychopharmacology (Berl)* **2011,** *213*, 307-320.

27. Nic Dhonnchadha, B. A.; Fox, R. G.; Stutz, S. J.; Rice, K. C.; Cunningham, K. A. Blockade of the serotonin 5-HT2A receptor suppresses cue-evoked reinstatement of cocaine-seeking behavior in a rat self-administration model. *Behav. Neurosci.* **2009,** *123*, 382-396.

28. Doly, S.; Quentin, E.; Eddine, R.; Tolu, S.; Fernandez, S. P.; Bertran-Gonzalez, J.; Valjent, E.; Belmer, A.; Vinals, X.; Callebert, J.; Faure, P.; Meye, F. J.; Herve, D.; Robledo, P.; Mameli, M.; Launay, J. M.; Maldonado, R.; Maroteaux, L. Serotonin 2B Receptors in Mesoaccumbens Dopamine Pathway Regulate Cocaine Responses. *J. Neurosci.* **2017,** *37*, 10372-10388.

29. Cathala, A.; Devroye, C.; Robert, E.; Vallee, M.; Revest, J. M.; Artigas, F.; Spampinato, U., Serotonin2B receptor blockade in the rat dorsal raphe nucleus suppresses cocaine-induced hyperlocomotion through an opposite control of mesocortical and mesoaccumbens dopamine pathways. *Neuropharmacology* **2020,** *180*, 108309.

30. Czoty, P. W.; McCabe, C.; Nader, M. A. Effects of the 5-HT(1A) agonist (+/-)-8-hydroxy-2-(di-n-propylamino)tetralin (8-OH-DPAT) on cocaine choice in cynomolgus monkeys. *Behav. Pharmacol.* **2005,** *16*, 187-191.

31. Boateng, C. A.; Bakare, O. M.; Zhan, J.; Banala, A. K.; Burzynski, C.; Pommier, E.; Keck, T. M.; Donthamsetti, P.; Javitch, J. A.; Rais, R.; Slusher, B. S.; Xi, Z. X.; Newman, A. H. High Affinity Dopamine D3 Receptor (D3R)-Selective Antagonists Attenuate Heroin Self-Administration in Wild-Type but not D3R Knockout Mice. *J. Med. Chem.* **2015,** *58*, 6195-6213.

32. Kumar, V.; Bonifazi, A.; Ellenberger, M. P.; Keck, T. M.; Pommier, E.; Rais, R.; Slusher, B. S.; Gardner, E.; You, Z. B.; Xi, Z. X.; Newman, A. H. Highly Selective Dopamine D3 Receptor (D3R) Antagonists and Partial Agonists Based on Eticlopride and the D3R Crystal Structure: New Leads for Opioid Dependence Treatment. *J. Med. Chem.* **2016,** *59*, 7634-7650.

33. Pattison, L. P.; McIntosh, S.; Sexton, T.; Childers, S. R.; Hemby, S. E. Changes in dopamine transporter binding in nucleus accumbens following chronic self-administration cocaine: heroin combinations. *Synapse* **2014,** *68*, 437-444.

34. Pattison, L. P.; McIntosh, S.; Budygin, E. A.; Hemby, S. E. Differential regulation of accumbal dopamine transmission in rats following cocaine, heroin and speedball self-administration. *J. Neurochem.* **2012,** *122*, 138-146.

35. McIntosh, S.; Sexton, T.; Pattison, L. P.; Childers, S. R.; Hemby, S. E. Increased Sensitivity to Cocaine Self-Administration in HIV-1 Transgenic Rats is Associated with Changes in Striatal Dopamine Transporter Binding. *J. Neuroimmune Pharmacol.* **2015,** *10*, 493-505.

36. Hemby, S. E.; Co, C.; Dworkin, S. I.; Smith, J. E. Synergistic elevations in nucleus accumbens extracellular dopamine concentrations during self-administration of cocaine/heroin combinations (Speedball) in rats. *J. Pharmacol. Exp. Ther.* **1999,** *288*, 274-280.

37. Hemby, S. E.; Smith, J. E.; Dworkin, S. I. The effects of eticlopride and naltrexone on responding maintained by food, cocaine, heroin and cocaine/heroin combinations in rats. *J. Pharmacol. Exp. Ther.* **1996,** *277*, 1247-1258.

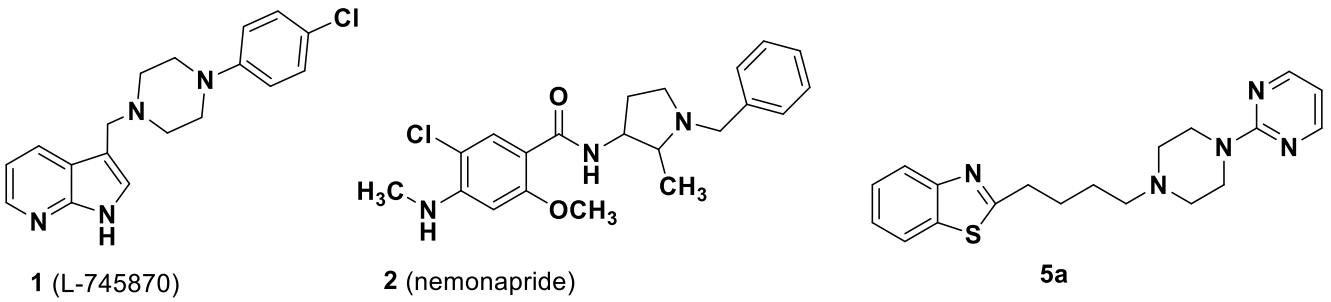

Figure 1. The structure of previous D_4R ligands.

Scheme 1. Synthesis of substituted or unsubstituted benzothiazole analogues[a]

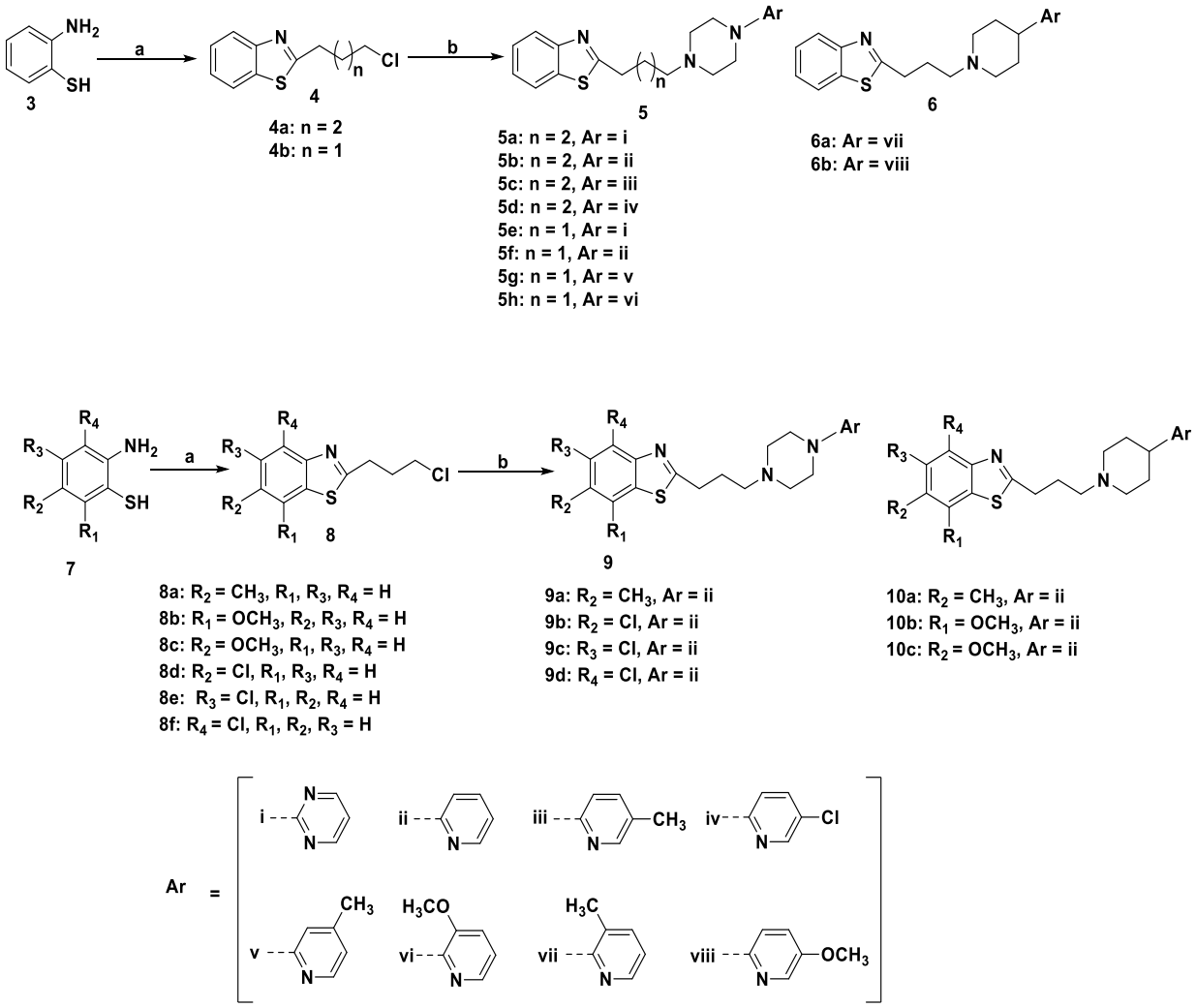

[a] Reagents and Conditions: (a) Toluene, 5-chloro pentanoyl chloride or 4-chloro butanoyl chloride, RT; (b) CH_3CN, KI, K_2CO_3, Reflux, appropriate arylpiperazine or arylpiperidine.

Table 1. Human dopamine D_2-like receptor competition binding in HEK293 cells for Benzothiazole analogues with varying 3 or 4-carbon linker chains.

Compound	Structure	cLogP	PSA	D_2R	D_3R	D_4R	Selectivity D_2R/D_4R	Selectivity D_3R/D_4R
				K_i (nM) ± SEM				
5a[13]	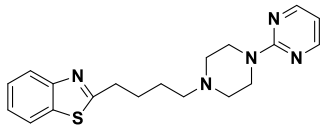	3.39	43.6	127 ± 10	93.2 ± 8.3	3.05 ± 0.16	42	31
5b	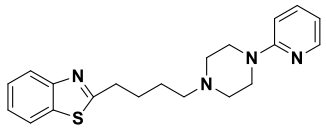	4.15	31.2	408 ± 21	58.5 ± 1.2	9.85 ± 2.01	41	6
5c	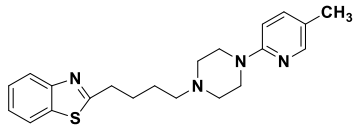	4.53	31.2	1050 ± 170	205 ± 3	21.2 ± 1.4	50	10
5d	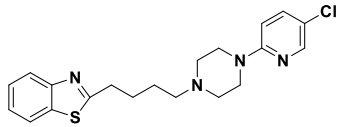	4.83	31.2	830 ± 160	104 ± 4	4.85 ± 0.57	171	21
5e[13]	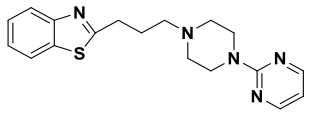	2.86	43.5	6370 ± 1020	1650 ± 120	6.52 ± 0.61	977	253
5f	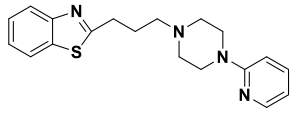	3.63	31.2	2930 ± 170	1150 ± 190	2.21 ± 0.01	1326	520

5g	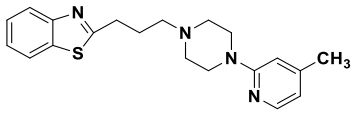	4.01	31.2	1580 ± 470	1320 ± 690	2.89 ± 0.95	547	456
5h	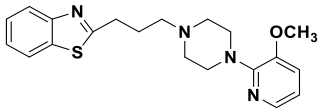	3.93	40.4	519 ± 211	288 ± 194	1.74 ± 0.58	298	165
6a	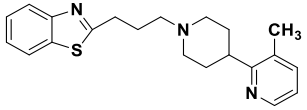	3.99	27.9	13,300 ± 9000	773 ± 213	26.0 ± 13.4	510	30
6b	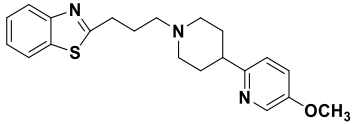	3.96	37.2	17,400 ± 8500	4860 ± 3870	24.8 ± 2.6	699	196
9a	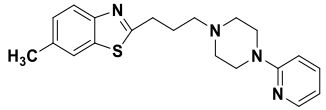	4.12	31.2	49,800 ± 42,700	201,000 ± 164,000	59.0 ± 45.4	844	3403
9b	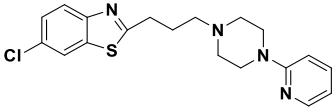	4.37	31.2	2420 ± 160	222 ± 141	27.2 ± 10.0	89	8
9c	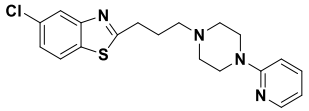	4.37	31.2	14,000 ± 10,600	1550 ± 670	11.5 ± 5.9	1214	135

9d	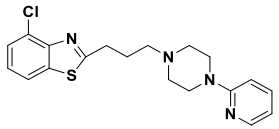	4.37	31.2	6500 ± 5220	512 ± 351	36.7 ± 7.7	177	14
10a	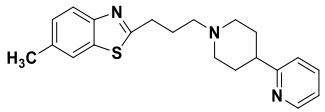	4.21	27.9	6890 ± 4680	11,800 ± 9500	45.8 ± 28.6	150	257
10b	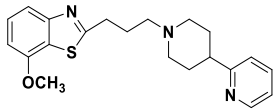	4.00	37.2	669 ± 354	228 ± 82	21.3 ± 7.6	31	11
10c	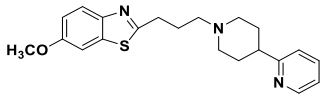	4.00	37.2	427 ± 189	7200 ± 5040	6.12 ± 4.06	70	1177

[a] K_i values determined by competitive inhibition of [^{3}H]*N*-methylspiperone binding in membranes harvested from HEK 293 cells stably expressing hD_2R, hD_3R, or hD_4R. All K_i values are presented as means ± SEM.

Table 2. D_2R- and D_4R-mediated effects on cAMP production. Compounds were tested alone (agonist mode) and with an EC_{80} concentration of dopamine (antagonist mode) for their ability to alter cAMP production mediated by D_2R and D_4R signaling.

	D_2R				D_4R				EC_{50}	IC_{50}
Compound	**cAMP E_{max} %[a]**	**cAMP EC_{50} (nM)[b]**	**cAMP Ant. %[a]**	**cAMP IC_{50} (nM)[b]**	**cAMP E_{max} %[a]**	**cAMP EC_{50} (nM)[b]**	**cAMP Ant. %[a]**	**cAMP IC_{50} (nM)[b]**	**Selectivity D_2R/D_4R**	**Selectivity D_2R/D_4R**
5a	Inactive	inactive	97.6 ± 5.1	353 [207 - 605]	inactive	inactive	97.9 ± 2.3	31.8 [24.7 - 40.9]	ND	11
5b	59.4 ± 3.0	124 [68.9 - 222]	ND	> 100000	inactive	inactive	95.6 ± 2.3	123 [95.9 - 157]	ND	ND
5c	Inactive	inactive	107 ± 5	2010 [1390 - 2910]	inactive	inactive	106 ± 3	600 [467 - 771]	ND	3.4
5d	Inactive	inactive	ND	ND	inactive	inactive	ND	10800 [7520 - 15500]	ND	ND
5e	80.9 ± 6.9	1180 [577 - 2390]	ND	> 100000	14.0 ± 0.8	4.34 [1.1 - 17.1]	82.2 ± 2.0	32.3 [24.7 -42.2]	272	ND
5f	37.5 ± 3.2	936 [483 - 1770]	81.3 ± 4.5	6690 [4120 - 11000]	14.2 ± 1.2	10.6 [1.6 - 64.8]	78.8 ± 2.3	69.3 [50.9 - 94.5]	88	97
5g	Inactive	inactive	92.8 ± 4.9	628 [375 - 1040]	inactive	inactive	88.0 ± 4.4	27.8 [15.3 - 49.2]	ND	23
5h	Inactive	inactive	86.4 ± 4.4	185 [105 - 327]	inactive	inactive	90.4 ± 2.6	30.6 [23.1 - 40.6]	ND	6.0
6a	Inactive	inactive	104 ± 6	4530 [2740 - 7500]	inactive	inactive	97.6 ± 4.5	67.2 [41.2 - 109]	ND	67
6b	Inactive	inactive	98.3 ± 5.8	2340 [1350 - 4060]	inactive	inactive	102 ± 5	173 [105 - 284]	ND	14
9a	53.6 ± 4.3	591 [283 - 1210]	79.4 ± 6.9	3660 [1710 - 7860]	13.1 ± 2.2	29.5 [1.5 - 29.3]	77.0 ± 3.5	328 [211 - 506]	20	11
9b	50.2 ± 8.0	1620 [544 - 4320]	ND	ND	32.3 ± 2.5	272 [110 - 646]	71.1 ± 4.2	1750 [1020 - 2990]	6.0	ND
9c	78.3 ± 6.0	1800 [1004 - 3227]	ND	11600 [5310 - 25500]	inactive	inactive	73.0 ± 4.0	816 [454 - 1470]	ND	14
9d	84.5 ± 9.7	2050 [871 - 4760]	62.4 ± 7.8	3040 [629 - 10800]	inactive	inactive	67.7 ± 5.0	1670 [839 - 3320]	ND	1.8
10a	27.0 ± 3.1	496 [165 - 1500]	89.9 ± 5.7	719 [380 - 1340]	24.2 ± 2.1	150 [42.3 - 593]	77.0 ± 5.7	87.6 [42.6 - 180]	3.3	8.2
10b	42.4 ± 5.1	183 [45.2 - 649]	92.9 ± 4.7	1840 [1160 - 2950]	11.3 ± 1.2	12.7 [2.6 - 58.1]	86.0 ± 4.7	85.5 [46.3 - 158]	14	22
10c	65.3 ± 5.5	228 [102 - 488]	76.3 ± 5.8	2600 [1190 - 5490]	30.5 ± 2.1	38.6 [12.8 - 114]	86.4 ± 4.0	153 [96.3 - 242]	5.9	17

[a] Efficacy/antagonist % (Ant. %) values obtained from nonlinear regression of meaned data obtained from at least three independent experiments with triplicate measures. Values are presented as means ± SEM.

[b] Potency values obtained from nonlinear regression of meaned data obtained from at least three independent experiments with triplicate measures. Values are presented as mean [95% confidence interval].

ND, Not Determined due to an incomplete curve. Inactive, no measurable activity.

Table 3. D_2R-, D_3R-, and D_4R-mediated β-arrestin recruitment. Compounds were tested alone (agonist mode) and with an EC_{80} concentration of dopamine (antagonist mode) for their ability to alter β-arrestin recruitment to D_2R, D_3R, and D_4R.

	D_2R				D_3R				D_4R				EC_{50}		IC_{50}	
Compound	**β-arr E_{max} % [a]**	**β-arr EC_{50} (nM) [b]**	**β-arr Ant. % [a]**	**β-arr IC_{50} (nM) [b]**	**β-arr E_{max} % [a]**	**β-arr EC_{50} (nM) [b]**	**β-arr Ant. % [a]**	**β-arr IC_{50} (nM) [b]**	**β-arr E_{max} % [a]**	**β-arr EC_{50} (nM) [b]**	**β-arr Ant. % [a]**	**β-arr IC_{50} (nM) [b]**	**Selectivity D_2R/D_4R**	**Selectivity D_3R/D_4R**	**Selectivity D_2R/D_4R**	**Selectivity D_3R/D_4R**
5a	inactive	inactive	99.0 ± 3.4	242 [167 - 349]	21.1 ± 1.9	39.4 [10.6 - 147]	69.0 ± 7.4	1440 [766 - 2800]	inactive	inactive	100 ± 3	19.1 [13.9 - 26.4]	ND	ND	13	75
5b	32.0 ± 0.9	29.8 [18.6 - 47.6]	60.2 ± 4.3	849 [450 - 1600]	82.6 ± 5.3	17.8 [7.34 - 43.1]	inactive	inactive	inactive	inactive	97.8 ± 3.6	104 [71.1 - 153]	ND	ND	8.2	ND
5c	inactive	inactive	104 ± 4	1560 [1120 - 2170]	inactive	inactive	101 ± 8	937 [541 - 1630]	inactive	inactive	108 ± 4	275 [185 - 408]	ND	ND	5.7	3.4
5d	inactive	inactive	108 ± 19	23000 [8960 - 67700]	inactive	inactive	ND	ND	inactive	inactive	103 ± 4	414 [274 - 621]	ND	ND	56	ND
5e	29.9 ± 0.9	1060 [769 - 1470]	58.5 ± 6.5	10200 [4820 - 22500]	58.4 ± 1.8	2340 [1680 - 3260]	50.6 ± 15	15100 [4010 - 65800]	inactive	inactive	108 ± 4	71.5 [48.8 - 105]	ND	ND	143	211
5f	12.5 ± 0.5	1110 [710 - 1740]	94.6 ± 6.9	10000 [5890 - 17200]	47.7 ± 2.6	5560 [3440 - 8990]	56.4 ± 10	22000 [9050 - 60200]	inactive	inactive	105 ± 4	25.6 [17.5 - 37.4]	ND	ND	391	859
5g	inactive	inactive	102 ± 6	6430 [4010 - 10300]	inactive	inactive	101 ± 10	12900 [7490 - 22400]	inactive	inactive	88.6 ± 4.6	6.18 [2.59 - 17.6]	ND	ND	1040	2087
5h	inactive	inactive	94.0 ± 3.6	414 [268 - 633]	inactive	inactive	81.5 ± 3.4	474 [298 - 747]	inactive	inactive	91.7 ± 3.6	2.17 [1.41 - 3.40]	ND	ND	191	218
6a	inactive	inactive	100 ± 2	9920 [7660 - 12900]	inactive	inactive	101 ± 2	13300 [9450 - 18700]	inactive	inactive	100 ± 2	52.4 [40.3 - 68.3]	ND	ND	189	254
6b	inactive	inactive	107 ± 5.2	14300 [10500 - 19600]	inactive	inactive	112 ± 7	8460 [5590 - 12900]	inactive	inactive	100 ± 3	333 [244 - 454]	ND	ND	43	25
9a	37.1 ± 4.8	18900 [6600 - 56300]	89.6 ± 7.5	15600 [9330 - 26400]	60.5 ± 6.3	13100 [4130 - 38700]	64.9 ± 11	15300 [6270 - 41600]	8.9 ± 1.2	8.81 [1.15 - 112]	100 ± 6	2340 [1370 - 3950]	2148	1481	6.7	6.5
9b	ND	ND	75.2 ± 12	24200 [9680 - 65800]	ND	ND	inactive	inactive	inactive	inactive	93.9 ± 5.4	3260 [1970 - 5310]	ND	ND	7.4	ND
9c	ND	ND	ND	ND	ND	ND	32.8 ± 7.2	24000 [9070 - 76600]	inactive	inactive	104 ± 5	377 [221 - 631]	ND	ND	ND	64
9d	ND	ND	ND	ND	ND	ND	inactive	inactive	inactive	inactive	102 ± 6	2290 [1330 - 3860]	ND	ND	ND	ND
10a	inactive	inactive	92.5 ± 3.8	2780 [1980 - 3910]	inactive	inactive	97.0 ± 6.3	6700 [4330 - 10400]	inactive	inactive	98.6 ± 2.7	248 [187 - 237]	ND	ND	11	27
10b	inactive	inactive	98.3 ± 3.4	2260 [1660 - 3070]	inactive	inactive	107 ± 6	2770 [1820 - 4200]	inactive	inactive	103 ± 3	122 [86.5 - 172]	ND	ND	19	23
10c	29.0 ± 2.0	1170 [498 - 2890]	64.9 ± 3.7	4460 [2910 - 6810]	31.4 ± 2.5	3790 [1400 - 9660]	83.7 ± 8.6	8780 [4630 - 17100]	inactive	inactive	93.7 ± 3.0	724 [528 - 990]	ND	ND	6.2	12

[a] Efficacy/antagonist % (Ant. %) values obtained from nonlinear regression of meaned data obtained from at least three independent experiments with triplicate measures. Values are presented as means ± SEM.

[b] Potency values obtained from nonlinear regression of meaned data obtained from at least three independent experiments with triplicate measures. Values are presented as mean [95% confidence interval].

ND, Not Determined due to an incomplete curve. Inactive, no measurable activity.

Table 4. Psychoactive Drug Screening Program (PDSP) results from primary and secondary assays on an array of receptors and monoamine transporters. Receptors and transporters were initially tested with 10 μM **5f** and % inhibition measured compared to a known reference compound. Receptors and transporters with greater than 50% inhibition were selected for full assays to determine the affinity of **5f** for the receptor/transporter. Receptors with < 100 nM affinity for **5f** in bold.

Receptor / transporter	Primary screen (% inhibition)	Secondary assay K_i (nM)[c]
D1	59	2736
D2	39	NT
D3	72	584
D4	78	**9.48**
D5	-0.04	NT
5-HT1A	109	**5.80**
5-HT1B	68	2859
5-HT1D	75	1423
5-HT1E	60	2764
5-HT2A	98	**46.0**
5-HT2B	99	**13.0**
5-HT2C	73	3545
5-HT3	38	NT
5-HT5A	56	2266
5-HT6	3	NT
5-HT7	90	107
MOR	60	1265
DOR	8	NT
KOR	19	NT
Alpha1A	89	586
Alpha1B	89	397
Alpha1D	88	4262
Alpha2A	85	356
Alpha2B	85	358
Alpha2C	94	**72.0**
H1	85	431
H2	13	NT
H3	18	NT
H4	13	NT
Sigma 1 GP	85	252
Sigma 2	84	**72.7**
GABAA	35	NT
Beta1	32	NT
Beta2	39	NT
Beta3	22	NT
M1	3	NT
M2	11	NT
M3	15	NT
M4	21	NT
M5	13	NT
BZP Rat Brain Site	5	NT
PBR	9	NT
SERT	32	NT
NET	80	634
DAT	-14	NT

[c] NT – Not Tested due to > 50% inhibition in primary assessment.

Table 5. Functional assessment of **5f** and control compounds at 5-HT_{1A}, 5-HT_{2A}, and 5-HT_{2B} receptors in $G\alpha_i$ or $G\alpha_q$ calcium flux assays.

Receptor	Study mode	Ligand	EC_{50}/IC_{50} (nM)	Max response (% control)
5-HT_{1A}	Agonist	Serotonin	3.40	100
		5f	4600	58.8
	Antagonist	(S)-WAY-100635	6.60	100
		5f	>370*	37.4
5-HT_{2A}	Agonist	Serotonin	1.32	94.0
		5f	>10,000	0
	Antagonist	Altanserin HCl	5.27	101
		5f	532	106
5-HT_{2B}	Agonist	Serotonin	2.40	100
		5f	>10,000	14.1
	Antagonist	LY 272015 HCl	0.368	100
		5f	770	111

*370 nM was the highest concentration of **5f** that was not excluded by Eurofins in the $G\alpha_i$ assay as higher concentrations had agonist affects that interfere with interpretation of the antagonist assay.

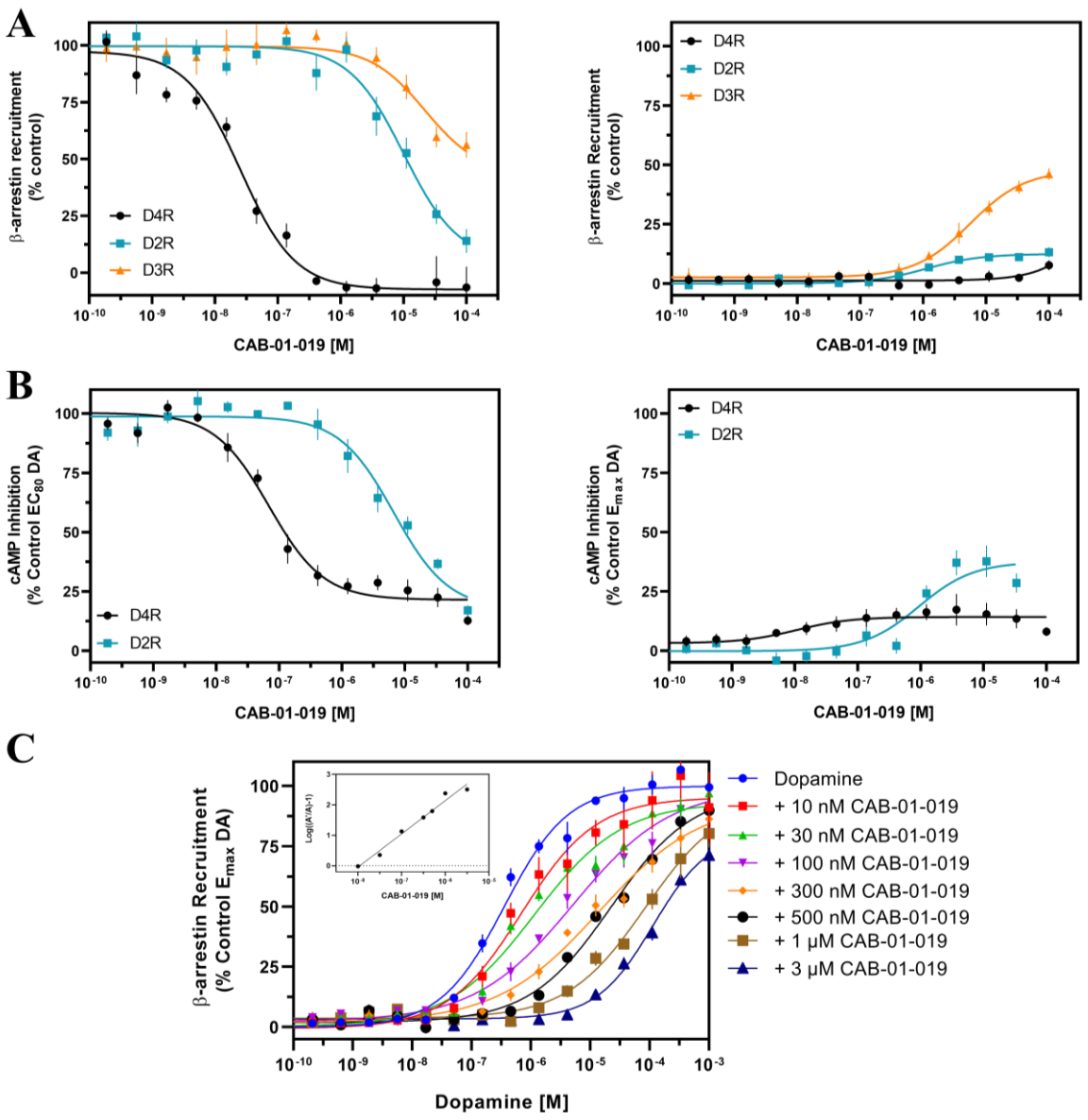

Figure 2. Lead compound 5f (CAB-01-019) demonstrated excellent D_4R selectivity in functional assays and is a competitive antagonist at D_4R. (**A**) **5f** is a potent full D_4R antagonist for β-arrestin recruitment with no D_4R agonist activity detected. At the D_2R and D_3R, **5f** has low potency in antagonist mode and is 391-fold and 859-fold selective for the D_4R, respectively (**Table 3**). The D_3R exhibits partial agonist activity with **5f** while the D_2R has very low partial agonist activity. **(B) 5f** potently antagonizes D_4R-mediated cAMP inhibition and is 97-fold more potent at the D_4R than the D_2R (**Table 2**). Further, **5f** has low efficacy D_4R agonism and is a low potency

partial agonist at the D_2R. (**C**) With increasing concentrations of **5f**, dopamine concentration-response curves are shifted to the right with no decrease in E_{max} indicating that **5f** is a competitive orthosteric ligand. Further, the Schild plot (inset) of these data had a slope of 1.09 and the K_b = 11.0 nM. All data are presented as means ± SEM from at least three independent experiments run in triplicate.

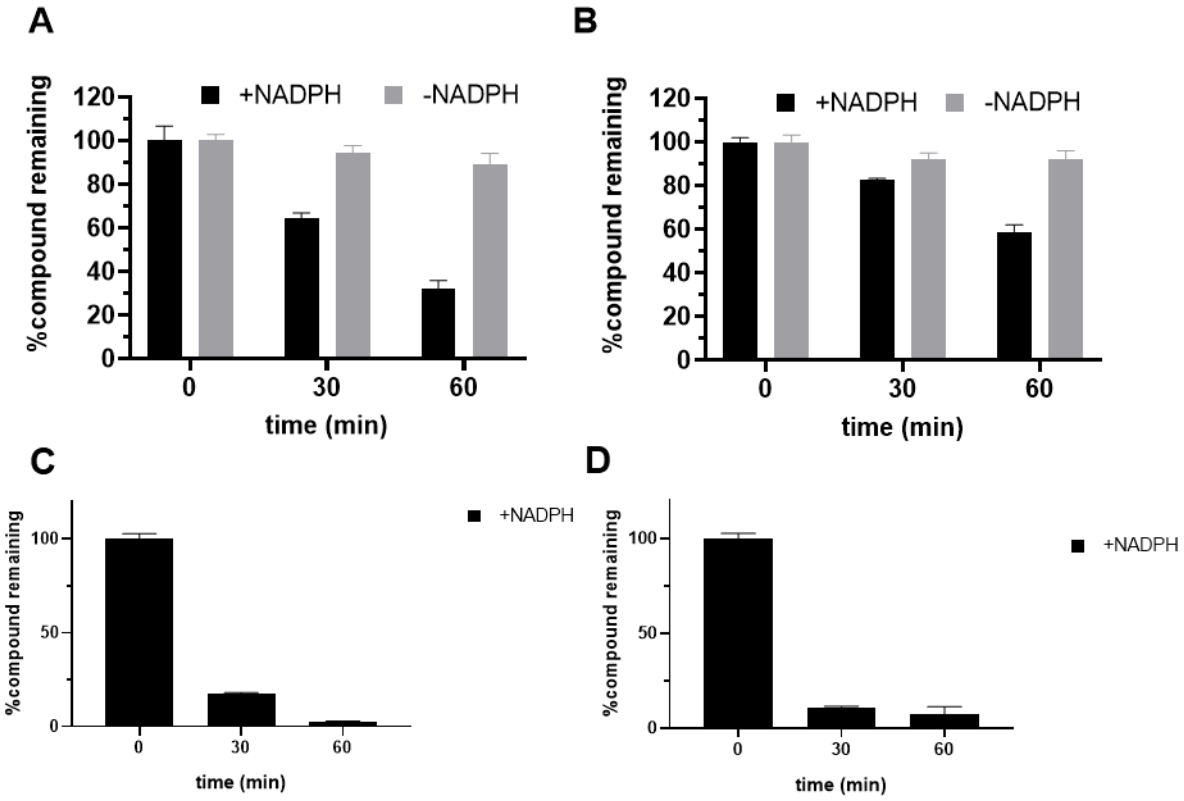

Figure 3. Phase I metabolic stability of **5f** in rat (**A**) and human (**B**) liver microsomes. **5f** shows time-dependent degradation in human and rat liver microsomes. **5f** was modestly stable in human liver microsomes. Data expressed as mean ± SEM, n = 3. As a positive control for Phase I metabolism, metabolic stability of buprenorphine in rat (**C**) and human (**D**) liver microsomes is also presented.

A

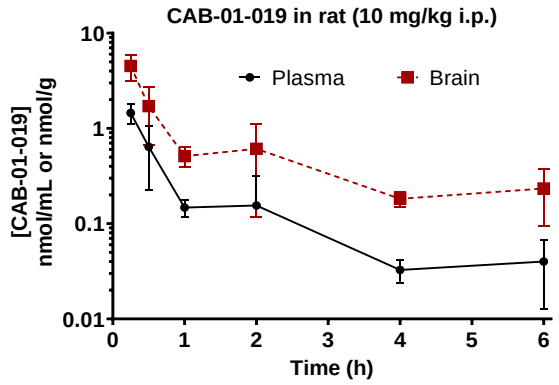

B

Tissue	C_{max} (nmol/ml or nmol/g)	T_{max} (h)	AUC_{0-t} (nmol*h/ml or nmol*h/g)	$t_{1/2}$ (h)	$AUC_{Brain/Plasma}$ Ratio
Plasma	1.45	0.25	1.05	0.82	3.5
Brain	4.52	0.25	3.67	1.09	

Figure 4. (A) Time-dependent *in vivo* pharmacokinetic analysis of **5f** (**CAB-01-019**) in Sprague Dawley (SD) rats following intraperitoneal (i.p.) administration of 10 mg/kg **5f**. Data expressed as mean ± SEM, n = 3 for each time point. **(B**) Calculated pharmacokinetics parameters of **5f** in rats.

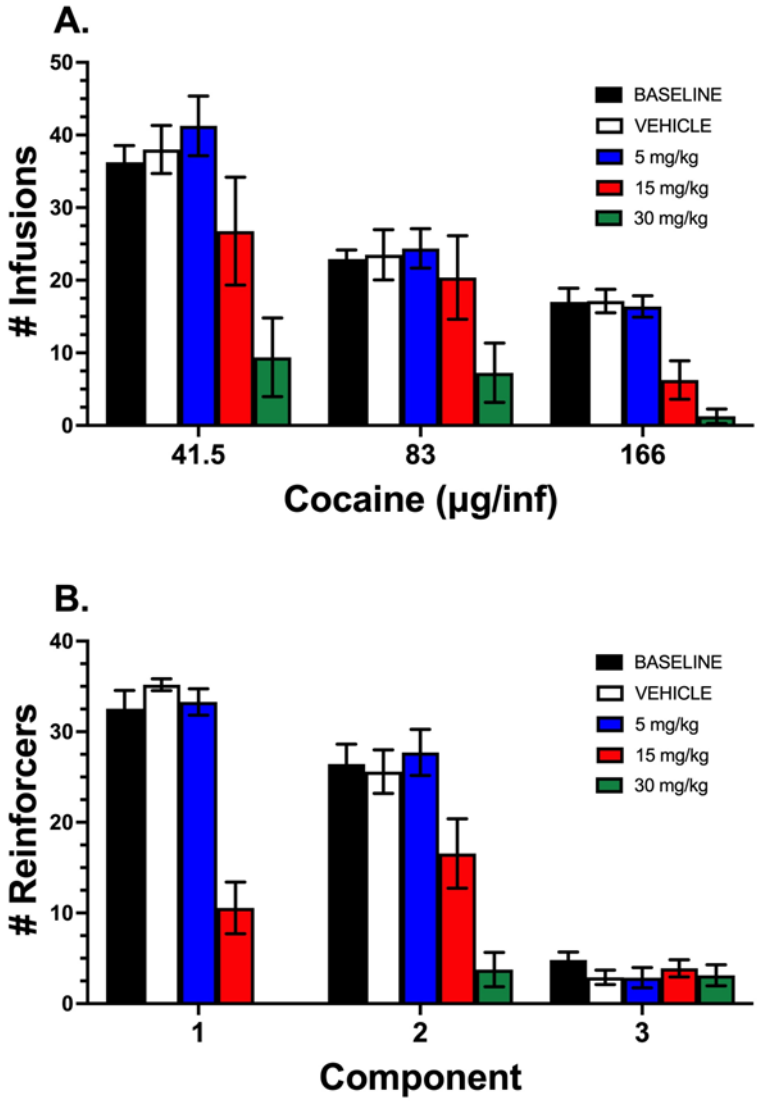

Figure 5: Effect of D_4R antagonist 5f on cocaine self-administration and food-maintained responding. (A). Number of infusions for each cocaine dose session at baseline, and following vehicle, 5, 15 and 30 mg/kg (i.p.) of **5f**. **5f** dose-dependently decreased intake at each cocaine dose in male Fisher F344 rats (n=8 per group). (**B).** Number of food reinforcers for each component at baseline, and following vehicle, 5, 15, and 30 mg/kg (i.p.) of **5f**. **5f** dose-dependently decreased food-maintained responding in male Fisher F344 rats (n=7-9 per group). Data expressed as mean ± SEM.